Validation of satellite-based noontime UVI with NDACC ground-based instruments: influence of topography, environment and satellite overpass time

Colette Brogniez[1], Frédérique Auriol[1], Christine Deroo[1], Antti Arola[2], Jukka Kujanpää[3], Béatrice Sauvage[1*], Niilo Kalakoski[3], Mikko R.A. Pitkänen[2], Maxime Catalfamo[1], Jean-Marc Metzger[4], Guy Tournois[5], Pierre Da Conceicao[5]

[1] Laboratoire d'Optique Atmosphérique, Université Lille 1 Sciences et Technologies, 59655 Villeneuve d'Ascq, France
[2] Finnish Meteorological Institute, Yliopistonranta 1 F, P.O. Box 1627, FI-70211 Kuopio, Finland
[3] Finnish Meteorological Institute, Earth Observation Unit, P.O. Box 503, FI-00101 Helsinki, Finland
[4] UMS 3365 - OSU Réunion, Université de La Réunion, St-Denis de La Réunion, France
[5] UMS 3470 - OSU Pytheas, Observatoire de Haute Provence, St-Michel l'Observatoire, France
[*] No more at LOA

Correspondence to: Colette Brogniez (colette.brogniez@univ-lille1.fr)

Abstract. Spectral solar UV radiation measurements are performed in France using three spectroradiometers located at very different sites. One is installed in Villeneuve d'Ascq, in the north of France (VDA). It is an urban site in a topographically flat region. Another instrument is installed in Observatoire de Haute Provence, in the French Southern Alps (OHP). It is a rural mountainous site. The third instrument is installed in Saint-Denis, Reunion Island (SDR). It is a coastal urban site on a small mountainous Island in the Southern tropics. The three instruments are affiliated to the Network for the Detection of Atmospheric Composition Change (NDACC) and carry out routine measurements to monitor the spectral solar UV radiation and enable derivation of UV index (UVI). The ground-based UVI values observed at solar noon are compared to similar quantities derived from OMI/Aura and GOME-2/Metop-A satellite measurements for validation of these satellite-based products. The present study concerns the period 2009-September 2012, date of the implementation of a new OMI processing. The new version (v1.3) introduces a correction for absorbing aerosols that were not considered in the old version (v1.2). Both versions of the OMI UVI products are available before September 2012 and are used to assess the improvement of the new processing. On average, estimates from satellite instruments always overestimate surface UVI at solar noon. Under cloudless conditions the satellite-derived estimates of UVI compare satisfactorily with ground-based data: the median relative bias is less than 8 % at VDA and 4 % at SDR for both OMI-v1.3 and GOME-2, and about 6 % for OMI-v1.3 and 2% for GOME-2 at OHP. The correlation between satellite-based and ground-based data is better at VDA and OHP (about 0.99) than at SDR (0.96) for both space-borne instruments. For all sky conditions the median relative biases are much larger, with large dispersion for both instruments at all sites (VDA: about 12 %; OHP: 9 %; SDR: 11 %). Correlation between satellite-based and ground-based data is still better at VDA and OHP (about 0.95) than at SDR (about 0.73) for both satellite instruments. These results are explained considering the time of overpass of the two satellites, which is far from solar noon,

preventing a good estimation of the cloud cover necessary to a good modelling of the UVI. Site topography and environment are shown to have a non-significant influence. At VDA and OHP, OMI-v1.3 shows a significant improvement with respect to v1.2 that did not account for absorbing aerosols.

1 Introduction

Monitoring of UV solar radiation at the surface is a necessary and important task to characterize the impact of atmospheric composition change, which is the goal for example of the Network for the Detection of Atmospheric Composition Change (NDACC) and of the Global Atmosphere Watch Programme (GAW). Indeed UV radiation affects the biosphere having both benefits and risks (detrimental effects) whose relative importance depends strongly on latitude and season. Currently, approximately 30 sites in the northern hemisphere and only 8 in the southern hemisphere perform spectral UV measurements. Observations at northern mid-latitudes help complete geographical coverage from other sites. Observations from Reunion Island, close to the tropic of Capricorn, are useful as well because only few sites exist in the low latitudes.

Due to the scarcity of surface-based UV measurements, which results in sparse geographical coverage, satellite platforms are very useful since they provide global data. Surface UV radiation from satellite radiance measurements is retrieved via radiative transfer codes whose input data are ozone and aerosol contents, surface albedo and cloudiness. Some of these data are products of the instrument itself (ozone, cloudiness) while others come from climatologies (aerosol content, albedo). Differences between the data of the two satellite instruments that will be used in this work (OMI and GOME-2) are detailed below.

Despite their extensive geographical coverage, satellite-based (SB) data products are affected by measurement uncertainties, as are ground-based (GB) products. However, SB data are also affected by modelling uncertainties. Moreover due to their rather coarse spatial resolution, SB data sometimes do not capture fine scale phenomena. Overall, various sites are useful for assessing the satellite data products in various conditions, including various latitude, land cover, altitude and climate. However, validation exercises are difficult to achieve due to differences in temporal and spatial resolutions of GB and SB data products. Extensive comparison studies between surface UV provided by OMI and GB measurements have been previously made (Tanskanen et al., 2007, Buchard et al., 2008, Ialongo et al., 2008, Weihs et al., 2008). Those studies dealt with version 1.2 which did not account for the influence of absorbing aerosols, implying a positive bias in OMI product. The OMI product has been tentatively corrected by several methods (Kazadzis et al, 2009a, Arola et al., 2009, Buntoung and Webb, 2010, Antón et al., 2012). From the comparisons against GB measurements, the OMI surface UVI at sites with low amounts of absorbing aerosols has been shown to be an overestimation of 0–10%. Alternatively, at sites with significant influence from absorbing aerosols, OMI surface UVI show a larger positive bias of up to 50%. All these OMI validations, apart from Buntoung and Webb (2010), were conducted using data collected at the time of the satellite overpass. Currently only one validation study is available for GOME 2, but it only concerns daily doses (Kalakoski, 2009). For both satellite instruments the previous validations address data up to 2008, except Antón et al., 2012 for OMI. Muyimbwa et al., 2015 and

Bernhard et al., 2015 address more recent OMI data. In the present study validations are conducted using data at noon, when the UVI is maximum for cloud-free conditions, over a more recent period at three French sites, including a new southern site.

Saint-Denis site, Reunion Island, is characterized by the proximity of the ocean, a complex topography and by a frequent occurrence of orographic clouds forming at around midday. This site may be not representative of satellite pixel because a large part of the area contributing to the satellite measurement is over the ocean where the cloud cover is likely different from that over the mountainous island. Due to its tropical location (high sun elevation in summer and low total ozone column) the UV radiation level is very high. Overpass by OMI occurs in the afternoon and GOME-2 overpass occurs in the morning. The two other metropolitan sites are characterized by the presence of absorbing aerosols, on average in larger quantity in Villeneuve d'Ascq than in Observatoire de Haute Provence, but less absorbing. Their mid-latitude situation implies lower UV radiation levels than in the tropics (lower sun elevation in summer and larger total ozone column). For both sites, overpass occurs close to noontime for OMI and in the morning for GOME-2.

OMI and GOME-2 websites make available UVI data and maps at solar noon, when values are generally close to the maximum and more risky for health, therefore comparison with ground-based UVI is carried out in this study at noontime. Validations of satellite-based estimates with ground-based measurements are conducted under cloudless and all sky conditions during about four years, January 2009-September 2012, date of the implementation of a new OMI processing. The new version (v1.3) introduces a correction for absorbing aerosols that were not considered in the old version (v1.2). All the archive has been reprocessed with OMI v1.3, so both versions of the OMI UVI products are available before September 2012 and are used in this work to assess the effect of the absorbing aerosol correction.

The influence of the cloudiness assumed by each satellite algorithm on the SB-GB UVI comparison is discussed. The influence of the site topography and environment is studied as well.

The ground-based spectroradiometers and the OMI and GOME-2 instruments are described in Sect. 2 along with the methodologies for deriving surface UVI. Section 3 presents the comparisons between the satellite-based and the ground-based UVI in various conditions and comparisons between measured and modelled UVI for cloudless conditions. Conclusions are provided in Section 4.

2 Instruments

2.1 Ground-based

2.1.1 Description

The UV measurements used here come from three French stations: Villeneuve d'Ascq (50.61° N, 3.14° E, 70 m above sea level (a.s.l.), referred to as VDA in the following), Observatoire de Haute Provence (43.93° N, 5.70° E, 686 m a.s.l., referred to as OHP) and Saint-Denis, Reunion Island (20.9° S, 55.5° E, 85 m a.s.l., referred to as SDR). The three sites are each

equipped with a double monochromator Bentham DTMc300. The instruments are thermally regulated. They provide global irradiance spectra in the 280-450 nm wavelength range with a 0.5 nm sampling step and a Full Width at Half Maximum (FWHM) of about 0.5 nm. Scans are performed every fifteen minutes (at SDR and OHP in 2009-2010), or thirty minutes (at VDA and OHP in 2011-2012). Scan duration is about 5 minutes.

105

2.1.1 Data processing

The instruments are regularly calibrated with standard 1000W lamps traceable to National Institute of Standards and Technology. After calibration, the wavelength misalignment is corrected via a software tool developed at Laboratoire d'Optique Atmosphérique (Houët, 2003) and improved during an intercomparison campaign with the QASUME (Quality
110 Assurance of Spectral Ultraviolet Measurements in Europe, Gröbner et al., 2005) instrument held in 2010. The cosine correction (Bernhard and Seckmeyer, 1999) is then carried out leading to the "measured" irradiance I at wavelength λ.

The erythemally weighted UV, UV_{ery}, is obtained by integrating over the wavelength the irradiance I(λ) weighted by the erythema action spectrum A(λ). The erythema action spectrum used is from CIE (Diffey and McKinlay, 1987). The UV index is then derived by dividing UV_{ery} (in Wm^{-2}) by 25×10^{-3} Wm^{-2}.

115 Irradiance uncertainty is estimated relying on Bernhard and Seckmeyer (1999). It results from uncertainties in the absolute calibration (including spectral irradiance lamp uncertainty provided by the lamp supplier, imprecision of adjustments and wavelength misalignment) and in the field measurements (imprecision of diffuser horizontality, uncertainty in cosine correction and in wavelength shift correction). During the QASUME campaigns, held for the three instruments, biases were observed: on average about 10% for VDA and OHP instruments and 3% at SDR (local instrument measurements lower than
120 those of QASUME, reports available at http://www.pmodwrc.ch/wcc_uv/wcc_uv.php?topic=qasume_audit). Following these results, the VDA and OHP lamps have been recalibrated in July 2012 at the World Radiation Center, Davos, Switzerland, and all the data reprocessed. A NDACC intercomparison campaign held in July 2015 in Hanover, Germany, and further analysis have shown that the measurements are 3-4 % lower than the reference measurements, that is within the reference measurement uncertainty.

125 The SDR lamp irradiance has been adjusted to the QASUME irradiance (May 2013), and all the data reprocessed.

The irradiance uncertainty leads to an UVI uncertainty for a coverage factor $k = 2$ of 5.3 % at VDA and OHP and 5% at SDR. The remaining biases observed at VDA and OHP are thus within these uncertainties.

All instruments are affiliated with NDACC.

130 ### 2.2 Satellite-based

2.2.1 OMI

Description

The Ozone Monitoring Instrument (OMI) on the Aura platform, launched in July 2004 into a sun-synchronous quasi-polar orbit, is a nadir-viewing UV/visible spectrometer dedicated to the monitoring of atmospheric ozone, trace gases, aerosol, cloudiness and surface UV. OMI measures the solar radiation backscattered by the atmosphere with a spectral resolution of about 0.45 nm in the UV and a spatial resolution at nadir of 13 km (along track) x 24 km (across track) (Levelt et al., 2006). Thanks to the Aura orbit and the large OMI swath width of 2600 km, the daily geographic coverage is global.

Data processing

The OMI version 1.2 algorithm first estimates clear-sky surface UV irradiance via a radiative transfer model using total ozone column, derived from measurements of OMI itself via another dedicated algorithm, surface albedo provided by a climatology (Tanskanen, 2004), a high-resolution extraterrestrial solar spectrum and climatological profiles of ozone and temperature (Krotkov et al., 2002). Secondly, non-absorbing aerosols and cloud cover are accounted for as a correction factor to estimate the actual surface UV radiation. The cloud cover parameter used is the cloud optical depth (COD) determined from OMI measurements. For products estimated at local noontime, change in cloudiness between the OMI local overpass time and noontime is not taken into account. This modelling is performed for solar zenith angles (SZA) lower than 85º. Finally, UVI is derived from spectral irradiance.

OMI-derived UVI data used here come from the OMUVB product available for overpass sites from http://avdc.gsfc.nasa.gov/index.php?site=595385375&id=79.

According to earlier validation works performed with OMI version 1.2 (Arola et al., 2009, Kazadzis et al., 2009a and 2009b, Antón et al., 2012), a large part of the high positive bias between OMI-UVI and GB data is due to absorbing aerosols. The new version 1.3 accounts for absorbing aerosols via an aerosol climatology (Kinne et al., 2013), which is used in a correction factor (CF) applied to v1.2 UV estimates (Arola et al., 2009).

Uncertainty in OMI-derived UVI is due to uncertainties in the clear-sky irradiance modelling (depending on ozone, surface albedo) and in the cloud-aerosol correction factor. According to Krotkov et al. (2002), the resulting uncertainty is about 5 % (10 % for $k = 2$) in clear sky conditions and about 7 % (14 %) in cloudy conditions. When the satellite overpass occurs at a time significantly different from local noon, an additional uncertainty is added because UVI is given at noontime and the correction factor estimated at the time of the overpass. In presence of absorbing aerosols, the estimated uncertainty for v1.2 increases to about 15-25 % (30-50 %), depending on aerosol type and load. In the latest version, this systematic overestimation has been significantly reduced. According to Arola et al. (2009), the use of the absorbing aerosol correction results in a significantly reduced bias by 5–20 %.

2.2.2 GOME-2

Description

The second Global Ozone Monitoring Experiment (GOME-2) on the Metop-A platform was launched on October 2006 into a sun-synchronous quasi-polar orbit. The spectrometer is nadir-scanning measuring the solar radiation backscattered by the atmosphere with a spectral resolution of about 0.27 nm in the UV. In the default scanning mode, the swath width is 1920 km enabling global coverage in 1.5 days. The spatial resolution is 40 km (along track) x 80 km (across track). The spatial resolution is kept constant throughout the swath by adjusting the speed of the scanning mirror (Munro, 2015).

Data processing

The GOME-2 algorithm proceeds similarly to OMI algorithm, with slight differences. Surface UV irradiance is estimated via a radiative transfer model using total ozone column, derived from GOME-2 measurements via another dedicated algorithm, surface albedo from the same climatology as the OMI algorithm, an extraterrestrial solar spectrum, climatological profiles of ozone, temperature, aerosols and clouds (Kujanpää and Kalakoski, 2015). Aerosol properties come from Global Aerosol Data Set (GADS) data (Koepke et al., 1997) and aerosol optical thickness comes from the climatology of Kinne (2007). Instantaneous cloud optical thickness (COD) is derived via interpolation of COD retrieved from measurements of AVHRR-3/Metop-A (which is on the same platform as GOME-2, having a morning orbit and the same local overpass time) and AVHRR-3 aboard NOAA satellites on the afternoon orbit (NOAA-18 until 3 June 2009, and then on NOAA-19). Depending on the station latitude, two or more AVHRR overpasses occur making two or more COD values available. All input data are mapped to a regular 0.5 º x 0.5 º latitude-longitude grid. UVI is derived from spectral irradiance and given on the same grid.
For the current study, O3M SAF offline surface UV (OUV) products were reprocessed using the algorithm version 1.13 with a special option to store diurnal COD values, which are not included in the standard product.
Uncertainty in GOME-2-derived UVI is due to uncertainty in the irradiance modelling (depending on ozone, surface albedo, cloud and aerosols). The resulting uncertainty is about 8 % (16 %) in clear sky conditions and about 10-20 % (20-40 %) in cloudy conditions, depending on the number of COD values available. As for OMI, the largest contribution to the uncertainty comes from the cloudiness estimate because UVI is given at noon rather than at the satellite overpass time. In presence of absorbing aerosols, the uncertainty increases to about 30-35 % (60-70 %), depending on aerosol type and content (Kujanpää, 2013).

3 Results

Due to their limited spatial resolution, space-borne measurements represent an average value for the observed pixel. Thus, when the cloud cover is not homogenous in the pixel, satellite data should not be directly compared to instantaneous ground-based measurements. For comparison at overpass time, the effect of the cloud variability within a satellite sensor pixel can be accounted for by averaging GB measurements over a time interval around the time of overpass. Here, comparisons are conducted at noontime, and the cloudiness used in OMI and GOME-2 algorithms are not actual values at noontime.

Nevertheless, for all sky conditions (AS), GB UVI have been averaged over a time interval around noontime. Several time intervals have been tested and hourly average of GB values has been selected as being better representative of spatial measurements for both space-borne instruments. Though GOME-2 pixel is larger than OMI pixel a mean over a larger time interval is not valuable since it would introduce a low bias in the GB product at solar noon (indeed, UVI is generally maximum at noon).

For cloudless conditions (CS), to avoid introducing a low bias in the GB product at solar noon (see above), no average was calculated. The selection of CS measurements at noontime cannot be made via cloud information available in the OMI data files since the COD corresponds to overpass time, for GOME-2 cloud information is interpolated at noon from AVHRR data (see section 2.2.2), therefore the COD value maybe not really valid. Thus, CS selection is based on the examination of the GB-UVI measurements. Two criteria are set up to declare the sky as "cloudless": (i) the shape of the curve of the UVI diurnal variations around noon must be smooth (visual inspection), and (ii) the UVI relative dispersion around the hourly mean must be less than 5 %, this value being an estimate of the UVI variation due to SZA variation around noontime (estimation derived from modelling). This second criterion is checked automatically. In addition, images from the SEVIRI sensor on the MSG satellite must show cloud free conditions close to the measurement time. This method is not perfect because a nearly constant thin cloud cover can be mistaken for cloud free.

We have considered two limits (100 and 10 km) for the distance between the GB station and the cross track position (CTP) for OMI and the grid cell centre point for GOME-2.

Satellite-based and ground-based datasets are compared by computing the UVI difference (SB-GB), the UVI relative difference (SB-GB)/GB) expressed in per cent, and by plotting correlation diagrams of UVI. The following statistics parameters are used to quantify the agreement: mean and root-mean square of the difference, mean, root-mean square and standard deviation of the relative difference. Since the difference/relative difference distributions are skewed we have also used the median and the 10^{th} and 90^{th} -percentiles. All these quantities are defined in the Appendix. In addition, the correlation coefficient and the equation of the regression line obtained via a bivariate method (York et al., 2004) are estimated. These statistical parameters are common in such validation studies (for example: Tanskanen et al., 2007, Ialongo et al., 2008, Weihs et al., 2008, Kalakoski, 2009, Kazadzis et al., 2009a, Muyimbwa et al., 2015, Bernhard et al., 2015).

The comparisons between SB and GB UVI are first carried out considering all the UVI pairs for each satellite sensor for 100 km limit distance. In order to interpret the biases observed, radiative transfer calculations are performed for cloudless conditions. Then, other comparisons are made for 10 km limit distance and with a filter on altitude. Finally, to enable a comparison of the performances of the satellite sensors an additional study restricted to common dates is conducted.

3.1 VDA

At this northern mid-latitude site, OMI overpasses occur from 0.5 h before to 2.5 h after solar noon. The GOME-2 overpasses take place in the morning from 3 h to 0.5 h before solar noon. VDA site, located in a topographically flat region,

is characterized by rather high total ozone columns (on average in the 250-450 DU range) and by the presence of absorbing aerosols of pollutant origin. The surface albedo at 360nm, provided in the OMUVB database, exhibits a weak seasonality in the [0.03-0.07] range.

For both satellite instruments, the distance between the ground station and the CTP/grid cell centre point is first chosen smaller than or equal to 100km.

Comparison results for AS conditions are shown in Fig. 1 for both satellite instruments, the upper panels present OMI-v1.3, and the lower panels GOME-2. Histograms of the per cent relative differences between SB and GB UVI data are located to the left and correlation diagrams are located to the right. Crosses circled with blue (for OMI) or turquoise (GOME-2) correspond to COD less than or equal to 1. Notice that the GOME-2 data set is smaller than the OMI data set because there is only one value per day and no value when SZA at noon is larger than 70°. The data show a medium dispersion around relative difference means (STD nearly 40 %, means nearly 21 %), the correlation between SB and GB UVI is strong (correlation coefficients $r \sim 0.95$) and the regression lines have a slope larger than unity (1.08 ± 0.01 for OMI, 1.12 ± 0.01 for GOME-2) with a small intercept. Satellite-derived UVI is larger than GB-derived UVI (positive relative difference) in 78 % of cases for OMI and in 73 % for GOME-2. When the COD is smaller than or equal to 1 (circled crosses) the UVI relative difference is almost always positive for OMI (Fig 1b), but is less so for GOME-2 (Fig. 1d). Satellite-derived UVI smaller than GB-derived UVI (negative relative difference) can occur when the COD is large, as seen in Fig. 3a and 3c where the UVI relative difference is plotted versus the COD retrieved from satellite instruments. These negative UVI relative differences for large COD are observed for both low and high UVI (UVI ≥ 3: blue circles for OMI, green circles for GOME-2), especially for OMI. Negative UVI differences for small COD (COD ≤ 1) are sometimes observed for GOME-2, which can be related to the SZA at the time of satellite overpass. Indeed, as seen in Fig. 4a and 4c, a filter set up on SZA at overpass shows that SZA > 60° corresponds to UVI < 3 and to many negative relative differences for both OMI and GOME-2 (blue and green circles). Approximate values of the median relative biases are 12.5 % for OMI and 12.1 % for GOME-2. The 90-th percentiles (p_{90}) indicate that 10 % of the cases correspond to relative differences larger than about 71% and 64 % for OMI and GOME-2 respectively (Fig. 1 caption). These 10 % cases for which the SB UVI overestimate the UVI at the surface are identified as red and violet crosses in Fig. 3a and 3c, i.e. correspond often to UVI lower than 3 and to a large COD. The 10-th percentiles (p_{10}) indicate that 10 % of the cases correspond to OMI and GOME-2 underestimate of more than about 15 % (Fig. 1 caption), associated also to UVI < 3 and to a large COD (Fig. 3a and 3c).

Figure 2 shows the results obtained for CS conditions. The dispersion around relative difference means is weak (STD < 10 %, means < 8 %), the correlations between SB and GB UVI are very strong ($r \sim 1$), and the slopes of the regression lines are slightly larger than for AS conditions (1.10 ± 0.01 for OMI, 1.14 ± 0.02 for GOME-2) with small intercepts. Satellite-derived UVI is still generally larger than GB-derived UVI (~ 92 % of cases for OMI, 80 % for GOME-2) and this corresponds almost always to COD ≤ 1 (circled crosses), as seen also in Fig. 3b and 3d. These low COD indicate that the satellite algorithms provide a good estimate of the actual cloudiness. As for GOME-2 for AS conditions, for UVI values

smaller than about 3 GOME-2 values are generally smaller than GB values (Fig. 3d), and these cases correspond to SZA > 60° (Fig. 4d). Only two such cases are observed for OMI (Fig. 3b and 4b). Both satellite sensors demonstrate a positive median relative bias (SB-UVI > GB-UVI) of about 8.5 %. The number of CS cases is not very large for GOME-2 comparison (37), but the results are statistically robust. 10 % of the cases correspond to a SB overestimate of more than 16 % and 13 % for OMI and GOME-2 respectively (p_{90}, Fig. 2 caption). p_{10} indicate that 10 % of the cases correspond to an OMI underestimate (p_{10} = 0 %, i.e. 10 % of the cases show a negative relative difference) and to more than 10 % GOME-2 underestimate. For GOME-2 most of these cases correspond to UVI < 3 (violet crosses in Fig. 3d).

The statistics of the results are reported in Table 1 for AS conditions and in Table 2 for CS conditions. The median bias is positive for both instruments and small: 0.21 for OMI and 0.33 for GOME-2 for AS conditions, 0.32 for OMI and 0.39 for GOME-2 for CS conditions.

A seasonal effect is observed on differences for both instruments with smaller values in winter, which correspond to small UVI. UVI relative differences for OMI show no seasonal effect (the large UVI differences being divided by high UVI). On the other hand, GOME-2 UVI relative differences exhibit seasonal variations, that is due to negative values related to small UVI and large SZA occurring mostly in winter rather than in other seasons (not shown). Surface albedo seasonality seems too weak to explain this behaviour.

These performances of the two satellite instruments should not be compared because the temporal coverage is not the same. Another study enabling to conduct a comparison of the performances is carried out further.

The overpass of both satellite instruments occurs sometimes quite far from noon. Surprisingly, no correlation between the UVI relative difference and the time difference between overpass and noon is observed, neither for AS nor for CS conditions (not shown).

For CS conditions, radiative transfer (RT) computations are carried out to understand the positive biases observed. We use DISORT (DIScret Ordinates Radiative Transfer) code for SZA < 70° (Stamnes et al., 1988, Van Weele et al., 2000). Apart from SZA, the extraterrestrial solar spectrum from Dobber et al. (2008), and Paur and Bass (1985) ozone cross-sections, we take for the input parameters: the total ozone column (TOC) from OMI (OMTO3), aerosol data from the sunphotometers of the AERONET/PHOTONS network (Holben et al., 1998, we use daily means (or monthly means) of the aerosol optical depth (AOD) at 440 nm, the Angström exponent (between 440 and 870 nm) to derive the spectral AOD, the single scattering albedo (SSA) at 440 nm) and the surface albedo from Feister and Grewe (1995). The other input parameters used in the RT model are the mid-latitude ozone, temperature and pressure profiles. Note that the sunphotometers are operating next to the spectroradiometers.

We have compared the simulated UVI to both OMI and GB UVI for several cloud-free cases. The histograms of the per cent relative difference between the computed UVI and the measured one are reported in Fig. 5a for GB UVI and 5b for OMI. GB UVI are 1.7 % lower and OMI UVI are 4.7 % higher than the simulated UVI, each value being within GB and OMI measurement uncertainty respectively. Since the TOC is the same for both modelling and OMI, this overestimation of OMI UVI might be mainly related to aerosol parameters and surface albedo, though this parameter value is small. Of course part

of the bias might come from differences between the two RT models used and also between the other input parameters. Kazadzis et al. (2009b) concluded also to an overestimation due to aerosol variability (in time and space). Of course we have to keep in mind that modelling computations are affected by uncertainties.

For this previous modelling we have chosen OMTO3 but other TOC data could be used, such as the TOC derived from the GB spectra following the method described in Houët and Brogniez (2004) relying on a differential absorption technique (Stamnes et al., 1988). The accuracy of this product is about 3 %. We find that this TOC is often larger than OMTO3, which is in agreement with Antón and Loyola (2011) findings for cloud-free conditions (OMTO3 smaller than GB-TOC by 2-3 % on average). Figure 5c shows the UVI relative difference between the computed and the GB UVI versus the TOC relative difference. The computed UVI is often larger than the GB UVI for a negative TOC relative difference, which could explain the positive 1.7 % bias. Note that the denominator of the relative differences (UVI or TOC) is the mean, contrarily to the SB – GB comparisons because, in this study, neither data is considered as a reference.

Another TOC product from OMI (OMDOAO3) exists, which is sometimes quite different from OMTO3 (either larger or smaller) leading to a different modelled UVI and thus to a quite different relative difference. For example a 7.6 % relative difference between GB UVI (4.8) and modelled UVI using OMTO3 (290 DU) becomes 4.8 % while using OMDOAO3 (297 DU).

TOC from GOME-2 is also sometimes different from OMTO3, and often smaller than spectroradiometer-TOC.

Underestimation of OMTO3 and of GOME-2 TOC for cloud-free and cloudy cases, as is found also by Antón and Loyola (2011), can explain part of the observed biases between SB and GB UVI. Aerosol climatology from Kinne et al. (2007, 2013) might also contribute to the biases. Indeed, these aerosol climatologies rely on AERONET data that show an interannual variability, and the gridding is 1ºx1º in latitude-longitude. Cloud cover variability within the satellite pixel (Kazadzis et al., 2009b) is expected to contribute to the biases as well as the surface albedo climatology from Tanskanen (2004).

The impact of the distance between the ground station and the CTP/grid cell centre point appears to be negligible. Tables 3 and 4 report results for distances smaller than or equal to 10 km. For both OMI and GOME-2, the number of UVI pairs (SB-GB) is much smaller than when considering 100 km distance. For AS conditions, the correlation between SB UVI and GB UVI data is hardly stronger for both satellite instruments (correlation coefficient increased by 0.01). Regression line slopes are closer to 1 than for 100 km case (1.06 ± 0.02 for OMI, 1.10 ± 0.03 for GOME-2). However, the relatively large uncertainties limit the significance of these differences. The values of the statistics parameters indicate an agreement close to that obtained for 100 km (median UVI relative bias for OMI of 10.3 % instead of 12.5 %, for GOME-2 14.3 % instead of 12.1 %). Based on p_{90} and p_{10} values, the filter on the distance has mainly removed cases of large SB UVI overestimate, not those of SB UVI underestimate (p_{90} < 53 %, much lower than for 100 km distance, p_{10} close to the 100 km ones).

For CS conditions correlation between OMI UVI and GB UVI is the same as for 100 km, the slope is almost unchanged (1.09 ± 0.01), the statistics parameters indicate better agreement (median relative bias 6.6 % instead of 8.4 %), though these results are statistically less robust than for 100 km because there are only 14 UVI pairs. As for AS conditions, few cases with

large SB overestimate have been removed (p_{90} about 10 %, p_{10} about -3 %). No study can be conducted for GOME-2 (only 2 pairs). Thus, a satellite validation performed with shorter distances between the satellite CTP/grid cell centre point and the GB instrument does not change significantly the results.

Finally, for AS conditions about 56 % of OMI and GOME-2 UVI data agree with GB data in the interval [-20 %; 20 %] (30 % agree in [-10 %; 10 %]). For CS conditions 100 % of OMI UVI data and 95 % of GOME-2 UVI data agree with GB data in the interval [-20 %; 20 %] (60 % agree in [-10 %; 10 %]).

As mentioned above, an additional study compares the performances of the two instruments on common dates. Tables 5 and 6 report the results. For AS conditions, the correlation between SB and GB UVI is strong ($r \sim 0.95$) for both satellite instruments, the slopes of the regression lines are significantly closer to 1 for OMI (1.05 ± 0.01) than for GOME-2 (1.12 ± 0.02), with a negative intercept for GOME-2. For CS conditions SB and GB UVI are very strongly correlated ($r \sim 0.99$) for both satellite instruments, the slopes of the regression lines are larger than for AS conditions with a smaller difference between OMI (1.10 ± 0.01) and GOME-2 (1.14 ± 0.02). The median biases and median relative biases are very close for both instruments for both AS and CS conditions. OMI and GOME-2 overestimates are the same for AS conditions (p_{90} about 65 %), but underestimate is smaller for OMI (p_{10} about -11 % for OMI, -17 % for GOME-2). For CS conditions, OMI essentially overestimates UVI (both p_{90} and p_{10} positive, only 7 % of the cases show a negative relative difference). GOME-2 is unchanged compared to the all-cases study (with underestimate corresponding to an UVI < 3).

The seasonal variability of differences between SB and GB UVI is greater for GOME-2 with frequently larger values than for OMI outside the winter period. UVI relative differences show no seasonal variability for OMI, but they do for GOME-2 because, as mentioned in the previous study, (i) the UVI differences for GOME-2 are larger than for OMI outside the winter season leading to larger relative differences for GOME-2 than for OMI and (ii) there are more negative relative difference for GOME-2 than for OMI, mainly in winter.

Tables 1 and 2 also report the results of the comparison of OMI-v1.2 data with GB data. The median UVI relative bias is about 21 % for AS conditions, overestimate is strong and underestimate is weak (p_{90} about 85%, p_{10} about -8 %). For CS conditions the median UVI relative bias is about 18 %, overestimate is large and there is almost no underestimate (p_{90} about 23 %, p_{10} about 10 %, only 3 % of the cases show a negative relative difference).

Median UVI biases are about 0.4 for AS conditions and about 0.8 for CS conditions. In addition the slopes of the regression lines are (1.17 ± 0.01) for AS conditions and (1.20 ± 0.01) for CS conditions. Apart from the strong correlation between SB and GB UVI (nearly the same as for v1.3), all these statistics parameters are significantly different from those produced by v1.3 and much worse. As expected, v1.3 data are more accurate than v1.2 data. Indeed, as observed in Fig. 6 (red dashed lines), the aerosol optical depth (AOD) is quite large (Fig. 6a) and the single scattering albedo (SSA) is significantly smaller than unity (Fig. 6b), leading to a correction factor (CF) applied to v1.2 data to account for absorbing aerosols (see section 2.2.1) much smaller than unity (Fig. 6c). As mentioned previously, UVI relative differences in v1.3 do not exhibit seasonal variability, whereas a weak seasonal variability is observed in v1.2 (not shown), possibly related to CF seasonality. The

current validation study at VDA demonstrates that v1.3 off-line correction for absorbing aerosol is very efficient, even if there remains a positive bias.

3.2 OHP

At this northern mid-latitude site, OMI overpasses occur from 0.25 h before to 2.75 h after solar noon and GOME-2 overpasses take place in the morning (ranging from 3.25 h to 1 h before solar noon). The OHP site, located in a mountainous region, is characterized by rather high total ozone columns (on average in the 250-420 DU range) and sometimes by the presence of absorbing aerosols. Surface albedo has a weak seasonal variability in the [0.02-0.05] range.

The first validation is conducted for distance between the GB station and the CTP/grid cell centre point ≤100 km.

Results for AS conditions are shown in Fig. 7. Similar to VDA, GOME-2 data set is limited because only one value per day is available. The data show medium dispersion around relative difference means (STD nearly 50 %, means nearly 21 %), GB and SB UVI are strongly correlated (r∼0.96) and regression lines have a slope larger than unity (1.04 ± 0.01 for OMI, 1.05 ± 0.01 for GOME-2) with a small intercept. Similar to VDA, satellite-derived UVI is generally larger than GB-derived UVI (82 % of positive relative difference for OMI, 72 % for GOME-2). When the COD is smaller than 1 the relative difference is almost always positive for OMI (Fig 7b), but is less so for GOME-2 (Fig. 7d). Negative differences for large COD are observed both for low and high UVI, especially for OMI data. Again, negative differences for small COD generally correspond to low UVI (Fig. 9a and 9c) and large SZA, especially for GOME-2 (Fig. 10a and 10c). Median values of the relative biases are about 9.3 % for OMI and 8.4 % for GOME-2. 10 % of the cases correspond to an SB overestimate larger than about 60 % (p_{90}) for both OMI and GOME-2 (Fig. 7 caption), cases identified as red and violet crosses in Fig. 9a and 9c, corresponding often to UVI < 3 and to a large COD, as observed at VDA. 10 % of the cases correspond to an SB underestimate of more than 8 % for OMI and 12 % for GOME-2 (p_{10}), associated also to UVI < 3 and to a large COD (Fig. 9c).

Figure 8 shows the results obtained for CS conditions. The dispersion around relative difference means is small (STD < 10 %, means < 6 %), SB and GB UVI are strongly correlated ($r = 0.99$), and the slopes of the regression lines are still larger than unity (1.05 ± 0.01 for OMI, 1.09 ± 0.01 for GOME-2). Note that the point well below the regression line in Fig 8b (red circled) corresponds to an OMI-CTP at 98 km distance from the GB site, 1700 m a.s.l. and to a large COD (7.75). Satellite-derived UVI is still often larger than GB-derived UVI (~ 85 % of cases for OMI, 68 % for GOME-2). The COD is generally small (Fig. 9b and 9d), indicating that the satellite algorithms perform a good estimate of the actual cloudiness. As was the case for all sky conditions, GOME-2 UVI are generally smaller than GB UVI for UVI values smaller than about 3 (green circles), these cases correspond to SZA > 60° (Fig. 10d). Few such cases are observed for OMI, they correspond to a UVI close to 1 (Fig. 10b). The positive median relative bias is 5.8 % for OMI and 4.1 % for GOME-2. SB overestimate is larger than 12 % for both OMI and GOME-2 in 10 % of the cases (p_{90}, Fig. 8 caption). p_{10} indicate that 10 % of the cases

correspond to an OMI underestimate and to more than 12 % GOME-2 underestimate. As previously, for GOME-2 these cases correspond to UVI < 3 (violet crosses in Fig. 9d).

The statistics of the results are reported in Tables 1 and 2. The median bias is positive and small for both satellite instruments: 0.32 for OMI and 0.41 for GOME-2 for AS conditions and about 0.25 for both OMI and GOME-2 for CS conditions.

As for VDA, seasonal variability is observed on differences for both satellite instruments with smaller values in winter. OMI relative differences show no seasonal variability, but GOME-2 relative differences exhibit seasonal variations not explained by the observed weak surface albedo seasonality.

Both satellite overpass times can be quite different from noon, however, no correlation between the relative difference and the time difference is observed (not shown).

As for VDA, we have performed RT calculations with also mid-latitude ozone, temperature and pressure profiles. Figures 5d and 5e show the histograms of the per cent relative difference between the computed UVI and the measured one for cloud-free conditions. GB and OMI UVI are 5.4 % and 2.2 % smaller than the simulated UVI respectively. This small underestimation of OMI UVI is well within OMI measurement uncertainty, and is caused, as for VDA, by differences between the input parameters (aerosol parameters, surface albedo, etc…) and between the two RT models used. Though rather large, the underestimation of GB UVI is still consistent with GB measurement uncertainty. This bias is explained considering the TOC value. Indeed, as at VDA, the TOC derived from the GB spectra is often larger than OMTO3. Figure 5f shows the UVI relative difference between the computed and the GB UVI versus the TOC relative difference. The modelled UVI is larger than the GB UVI for a negative TOC relative difference, which is consistent with the 5.4 % bias.

Similar to VDA, TOC from GOME-2 is also sometimes different from OMTO3, and often smaller than spectroradiometer-TOC (in agreement with Antón and Loyola (2011). Thus, part of the observed positive biases between SB and GB UVI for cloud-free and cloudy conditions can be explained by OMTO3 and GOME-2 TOC underestimation. At this site also, cloud cover variability within the satellite pixel (Kazadzis et al., 2009b), aerosol climatology (Kinne et al., 2013) and surface albedo climatology (Tanskanen, 2004) might explain part of the biases.

The results for distances between the ground station and the CTP/grid cell centre point ≤10 km are reported in Tables 3 and 4. The number of events is much smaller than for 100 km distance. For AS conditions, the slope of the regression line for OMI data is nearly unchanged compared to 100 km distance case (1.05 ± 0.02), the correlation coefficient and the parameters (median bias and median relative bias) as well. For GOME-2 though the slope of the regression line is closer to 1 compared to 100 km distance and the correlation coefficient nearly unchanged, the statistics parameters are slightly worse. p_{90} is much smaller for OMI (45 %), and unchanged for GOME-2 compared to that for 100 km distance, and p_{10} are close to the 100 km ones. That means that the filter on the distance has mainly removed cases of large OMI UVI overestimate.

For CS conditions, for both OMI and GOME-2, the regression slopes are not significantly different from those for 100 km distance, and the statistics of the results are very similar, except the GOME-2 p_{10} percentile (-19 %) meaning that the underestimate is stronger, though GOME-2 results are statistically less robust than for 100 km because there are only 19 UVI

pairs. Thus, the distance between the satellite CTP/grid cell centre point and the GB instrument does not affect significantly the results of the satellite sensor validation.

Since the region is mountainous, the effect of altitude may be evident in the data. The influence of altitude can only be studied with OMI data for which the terrain height is available in the OMUVB files. Tables 3 and 4 report the results accounting for CTP whose altitude is within +/- 250 m from the ground site altitude, this value being chosen as leading only to a +/- 2-3 % shift in erythemally weighted UV (McKenzie et al., 2001). Whether for AS or for CS conditions the statistics parameters are very close to those obtained without a filter on altitude, as well as the regression line slope and correlation coefficient. So, the altitude selection does not improve the comparisons between SB and GB data. This is likely due to OMI estimated cloudiness, to OMI spatial resolution and also to the fact that CTP with lower and higher altitude compared to the actual altitude of the site give opposite effects on UVI. Indeed all these factors play a role in the validations carried out with or without an altitude selection.

Finally, for AS conditions about 70 % of OMI UVI data and about 67 % of GOME-2 data agree with GB data in the interval [-20 %; 20 %] (44 % agree in [-10 %; 10 %]). For CS conditions about 97 % of both OMI and GOME-2 UVI data agree with GB data in the interval [-20 %; 20 %] (72 % agree in [-10 %; 10 %]).

The statistical comparisons restricted to the same dates for both OMI and GOME-2 are reported in Table 5 and 6. For AS conditions, the correlation between SB and GB UVI data is strong ($r \sim 0.96$) for both satellite instruments, the slopes of the regression lines are larger than 1, with no significant difference. For CS conditions the correlation is very strong ($r \sim 0.99$), the regression slope for OMI is slightly closer to 1 than for GOME-2. For AS conditions, median relative biases between GB and SB UVI data are very close for OMI and GOME-2, but median absolute bias for GOME-2 is larger than for OMI. For CS conditions, the median relative bias for GOME-2 is smaller than for OMI but median absolute bias for GOME-2 is larger than for OMI. This different behaviour between median relative bias and median bias for OMI and for GOME-2 is due to the seasonality of the relative differences and differences for GOME-2 - GB UVI pairs. Indeed, the seasonal variability of differences between SB and GB UVI is greater for GOME-2 than for OMI, and, as observed for VDA, OMI relative differences between SB and GB UVI show no seasonal variability, but GOME-2 relative differences do. OMI and GOME-2 overestimates are very close for AS conditions (p_{90} about 55 %), and underestimate is smaller for OMI (p_{10} about -8 % for OMI, -12 % for GOME-2). For CS conditions OMI mainly overestimates UVI (p_{10} = -0.5%), GOME-2 underestimate is much larger (p_{10} about -11 %).

The statistics of the results of the comparison for OMI-v1.2 are also reported in Tables 1 and 2. The median relative bias is about 20 % for AS conditions, v1.2 overestimates strongly and underestimates weakly UVI (p_{90} about 73%, p_{10} about 2%). For CS conditions the median UVI relative bias is about 17 %, overestimate is large and there is almost no underestimate (p_{90} about 23 %, p_{10} about 9 %, 3 % of the cases show a negative relative difference).

Median biases are about 0.8 for AS conditions and about 0.9 for CS conditions. The slopes of the regression lines are (1.14 ± 0.01) for AS conditions and (1.18 ± 0.01) for CS conditions. Thus, all these statistics parameters are significantly larger than those produced by v1.3, indicating that v1.3 product is more reliable than v1.2 one. This result can be understood

by looking in Fig. 6 (black dashed lines). AOD is quite large (Fig. 6a) and SSA significantly smaller than unity (Fig. 6b), leading to a CF applied to v1.2 UVI much lower than unity (Fig. 6c). The current validation study at OHP shows that the correction for absorbing aerosol performed in v1.3 is very efficient, though imperfect.

3.3 SDR

In the tropical region OMI overpasses occur in the afternoon from 0.75 h to 3.5 h after solar noon and GOME-2 in the morning from 4.25 h to 2.25 h before solar noon. As mentioned previously, SDR is characterized by rather low total ozone column (on average in the 240-300 DU range), by the proximity of the ocean, by a complex topography and by a frequent occurrence of clouds forming at around midday. Cloud variability between overpass time and noon is thus high, cloud subpixel variation is also high, and therefore, cloudiness estimation is the most important factor of uncertainty in deriving UVI from space measurements. This site may be not representative of satellite pixel because a large part of the area contributing to the satellite measurement is over the ocean where the cloud cover is likely different from that over the mountainous island. As at the other sites, surface albedo has a weak seasonality in the [0.04-0.08] range.

The first validation is conducted for distance between the GB station and the CTP/grid cell centre point ≤100 km.

Results for AS conditions are shown in Fig. 11. Similar to other sites, GOME-2 data set is limited because only one value per day is available. The data show large dispersion around relative difference means (STD nearly 57 %, mean nearly 29 % for OMI and STD nearly 67 %, mean nearly 35 % for GOME-2.). These dispersions and means are larger than at the two other sites. GB and SB UVI are correlated less strongly than at other sites ($r \sim 0.74$ for OMI, $r \sim 0.71$ for GOME-2), though the correlation is significant since the probability of getting by chance these r-values is lower than 0.05%. The slopes of the regression lines are much smaller than unity (0.91 ± 0.02 for OMI, 0.78 ± 0.03 for GOME-2). Satellite-derived UVI is generally larger than GB-derived UVI (~ 80 % of positive relative difference for both OMI and GOME-2). When the COD is smaller than 1 the relative difference is almost always positive for both instruments (Fig. 11b and 11d). Satellite-derived UVI smaller than GB-derived UVI can occur when the COD is large, as seen in Fig. 13a and 13c. No link with SZA at overpass is observed, indeed for OMI observations SZA is almost always smaller than 60º, and for GOME-2 several cases with SZA at overpass > 60º occur but the relative differences are not more negative than for other cases (not shown).

Median values of the relative biases are about 10 % for both OMI and GOME-2. The p_{90} indicate that 10 % of the cases correspond to an SB overestimate larger than about 86 % for OMI and 100 % for GOME-2 (Fig. 11 caption), these values are much larger than those observed at VDA and OHP. 10 % (p_{10}) of the cases correspond to SB underestimate of more that about 9 % for OMI and 6 % for GOME-2.

Figure 12 shows the results obtained for CS conditions. The dispersion around relative difference means is much lower than for AS conditions (STD < 9%, means < 4%), the correlations between SB and GB UVI are high, though weaker than at the two other sites ($r = 0.96$) and the slopes of the regression lines are close to unity (1.03 ± 0.02 for OMI, 0.98 ± 0.02 for GOME-2). Several SB-GB UVI pairs show negative relative difference, which correspond to COD >1. As seen in Fig. 13b

and 13d, the COD can still be large, indicating the difficulty for both satellite algorithms to estimate the actual cloudiness (i.e. here no cloud), though the possibility of a bad selection of CS cases at the GB site cannot be excluded. We have checked that the few points far from the regression line in Fig. 12b and 12d correspond to a large COD at overpass (for OMI) or at noon (for GOME-2). Satellite-derived UVI is larger than GB-derived UVI in nearly 70 % of cases for both instruments. The positive relative bias is nearly 4% for both OMI and GOME-2. 10 % of the cases (p_{90}) correspond to a SB overestimate of more than about 14 % for OMI and 11 % GOME-2 (Fig. 12 caption). The p_{10} percentiles indicate that only 10 % of the cases correspond to an OMI and GOME-2 underestimate larger than about 8 %.

All the statistics of the results are reported in Table 1 and in Table 2. The median bias is positive: about 0.8 for AS conditions and 0.4 for CS conditions for OMI, about 0.9 for AS conditions and 0.3 for CS conditions for GOME-2. These values are larger than at the two other sites for AS conditions because of the higher UVI levels.

A seasonal variability of the relative difference between GB and SB UVI is observed for both AS and CS conditions for GOME-2, but it seems to be related to the seasonality of the cloudiness rather than to the surface albedo seasonality (not shown).

As at the two other sites, though both satellite instruments overpass at times very far from noon, no correlation between the relative difference and the time difference is observed for AS and CS conditions (not shown).

Radiative transfer calculation results for cloud-free conditions, using tropical ozone, temperature and pressure profiles, are reported in Fig. 5. Figure 5g show that GB UVI is 3.3 % smaller than simulated UVI, and Fig. 5h that OMI UVI is 3.6 % larger, each bias being smaller than GB and OMI uncertainty respectively. As at the other sites, this overestimation of OMI UVI is due to differences between the input parameters other than TOC (aerosol parameters (though the aerosol load is small), surface albedo (though this parameter value is small), etc…) and between the two RT models used. Despite the underestimation of GB UVI is within the GB measurement uncertainty, it can be understood since, at this site also, the TOC derived from the GB spectra is often larger than OMTO3. Figure 5i shows the UVI relative difference between the computed and the GB UVI versus the TOC relative difference. GB UVI is often smaller than the computed UVI for a negative TOC relative difference, justifying the 3.3 % bias.

Part of the observed positive biases between SB and GB UVI for cloud-free and cloudy conditions can be explained by OMTO3 and GOME-2 TOC underestimation (according to Antón and Loyola (2011). At this site, aerosol climatology (Kinne et al., 2013) could not contribute much to the biases, since the aerosol load is small. Surface albedo climatology (Tanskanen, 2004) might contribute. According to Kazadzis et al., (2009b), due to the particular situation of SDR (coastal site in a small mountainous island) the cloud cover spatial variability in the satellite pixel should be the main contributor to the SB-GB UVI bias.

The study performed for distances (GB station - CTP/grid cell centre point) smaller than or equal to 10 km gives results similar to that at the two other sites (Tables 3 and 4). For AS conditions, OMI statistics parameters show a slight better agreement with GB data compared to 100 km distance case. The median relative bias is about 2% lower, p_{90} much smaller (by about 20 %)), though p_{10}, correlation between SB and GB UVI and regression line are nearly the same. For GOME-2,

statistics parameters show a worse agreement between SB and GB UVI compared to those for 100 km distance. The median relative bias is unchanged but p_{90} is larger (by about 15 %), p_{10} is lower (by about 2 %), correlation is weaker ($r \sim 0.60$) and the slope of the regression line is much smaller (0.62 ± 0.09). Finally, for AS conditions, the filter on the distance has removed cases of large SB UVI overestimate for OMI, for GOME-2 overestimate has become larger.

For CS conditions, OMI data compare slightly better with GB data than for 100 km case. The median relative bias is nearly unchanged, overestimate is lower (p_{90} lower by about 3 %) and underestimate is stronger (p_{10} lower by about 5 %). GOME-2 statistics parameters are little changed compared to 100 km distance, the GB and SB UVI data show the same strong correlation and the regression line slope (0.90 ± 0.07) is much smaller than for 100 km distance but the large uncertainty limits the significance of the difference. This latter case is statistically weakly robust because only 16 UVI pairs are available.

Thus, the comparison of surface UVI from OMI is little improved when smaller distance between the satellite CTP and the GB instrument is considered. For GOME-2 the comparison is worse for AS conditions.

Reunion Island is very mountainous so the effect of surface altitude may be evident in OMI comparison. Tables 3 and 4 show the results accounting for CTP whose altitude is within the sea level and +250 m above the site altitude. Whether for AS or CS conditions the statistics parameters are slightly worse, but not significantly, and correlation between SB and GB UVI data is similar. As for OHP site, an altitude selection does not lead to significant changes that is also likely due to the cloudiness estimate and to OMI spatial resolution.

Finally, for AS conditions about 62 % of both OMI and GOME-2 UVI data agree with GB data in the [-20 %; 20 %] relative difference interval (40 % agree in [-10 %; 10 %]). For CS conditions about 97 % of both OMI and GOME-2 data agree with GB data in the interval [-20 %; 20 %] (70 % and 80 % for OMI and GOME-2 respectively in [-10 %; 10 %]).

The statistical comparisons restricted to the same dates for both OMI and GOME-2 are reported in Tables 5 and 6. For AS conditions, the correlation between GB and SB UVI data is not very strong but it is better for OMI ($r \sim 0.74$ and $r \sim 0.70$ for OMI and GOME-2 respectively). The slopes of the regression lines are much smaller than 1, OMI slope being significantly closer to 1 (0.91 ± 0.03 for OMI, 0.78 ± 0.03 for GOME-2) and intercepts are both large and positive (larger for GOME-2). Median relative bias and absolute bias between GB and SB data are slightly smaller for OMI than for GOME-2. For CS conditions the correlations are strong and the same for both instruments ($r \sim 0.96$), both regression line slopes are close to 1 (OMI-slope >1, GOME-2-slope <1 with a positive intercept), but accounting for the uncertainties the difference is not significant. Median relative biases and absolute bias are slightly larger for OMI than for GOME-2. OMI overestimate is smaller than GOME-2 one for AS conditions (p_{90}), OMI underestimate is stronger than GOME-2 one (p_{10}). For CS conditions, OMI and GOME-2 p_{90} and p_{10} are very close.

As mentioned previously, GOME-2 relative differences between GB and SB UVI data show a seasonal variability related to cloud presence, while there is no variability for OMI.

The validation of previous OMI v1.2 UVI data with GB data does not show significant differences, as observed in Table 1 and 2. Indeed, for AS conditions the correlation between GB and SB UVI data is slightly weaker and the regression line

slope is slightly worse than for v1.3 data, but the other statistics parameters are very similar for both versions. For CS conditions, the correlation between GB and SB UVI data is slightly weaker and the regression line slope is nearly the same as for v1.3 data, but the other statistics parameters are worse. Overall, these changes are weak and not significant. The small difference between the v1.2 and v1.3 datasets is due to the small AOD (Fig. 6a, blue dashed line) and large SSA (Fig. 6b). Thus the correction factor at SDR is close to unity (Fig. 6c).

4 Conclusion

Validation of satellite noon-UVI products from OMI (v1.3) and GOME-2 (v1.13) with ground-based measurements of UVI at noon has been carried out at three sites. The three sites are very different regarding the topography and the environment. One is an urban site in a topographically flat region in the north of France (VDA). The second site is a rural mountainous site in the French Southern Alps (OHP). The third one is a coastal urban site on a small mountainous island in the southern tropics (SDR). Moreover the overpass of the two satellites occurs often far from solar noon at all sites, rendering the estimate of noon-UVI a challenge due to the difficulty to estimate the actual cloudiness at noontime. The sites are each equipped with spectroradiometers affiliated with the Network for the Detection of Atmospheric Composition Change.

SDR is difficult for spatial UV estimates because of (i) the mountainous topography of Reunion Island, and thus to the frequent formation of clouds at around midday and (ii) the satellite pixel covering both land and ocean, for which the cloud cover are likely different. The space-based total ozone retrieval and the cloud correction factor are affected which in turn affects the satellite-based UVI estimate, as observed by Antón and Loyola (2011) and by Kazadzis et al. (2009). The two other sites encounter less diurnal cloud cover variation and thus are expected to be more favourable for UV estimates. Nevertheless, these two latter sites are affected by aerosols caused by air pollution whose absorption should be accounted for in the satellite algorithms. Thus, aerosol and cloud cover inhomogeneities in the satellite pixel make the validation difficult at each ground-based site.

OMI-v1.3 UVI products, derived from v1.2 products using a correction factor to account for absorbing aerosols, show much better agreement with GB UVI measurements at VDA and OHP. The relative bias between SB and GB data is reduced by 8-12 %, in agreement with Arola et al. (2009).

On average, for both space-borne sensors, the median relative biases are in the [8.4 % - 12.5 %] and [3.8 % - 8.4 %] ranges for all sky and clear sky conditions respectively. Thus, accounting for the uncertainties in their UVI data (see Sect. 2), satellite-based and ground-based measurements agree for AS conditions and the agreement is good for CS conditions. We could even suggest that OMI and GOME-2 uncertainties (see sections 2.2.1 and 2.2.2 respectively) are overestimated.

For both all sky and cloud-free conditions the correlations are strong at VDA and OHP, meaning that the variability in actual UVI is retrieved in satellite-based estimates. At SDR the correlations are strong for cloud-free conditions and weaker for cloudy cases.

The 90th percentiles indicate that for all sky conditions, 10 % of the cases correspond to relative differences larger than about 70 % at VDA and OHP for both space-borne instruments. These 10 % cases correspond to UVI lower than 3, meaning that the comparisons are much better for high UVI than for low UVI. At SDR, for all sky conditions, 10 % of the relative differences are larger than about 85 % for OMI and 100 % for GOME-2. At SDR, UVI is often large so this strong overestimate is related to the site environment.

Underestimation of UVI by the space-borne instruments is more risky than overestimation for public health. The 10th percentiles indicate that 10 % of the cases have a relative difference lower than -17 % at VDA, -12 % at OHP and -10 % at SDR. For example, a 17 % underestimation for UVI = 6, means that the actual UVI value is 7, and a 10 % underestimation for a high UVI, i.e. UVI = 15, implies an actual value 16.5, which has more important consequences than overestimations. Though, these cases are not very frequent.

For the three sites, the distance between the ground-based site and the OMI cross tack position/GOME-2 grid cell centre point, as well as the environment topography are not critical, likely because of the rather coarse spatial resolution of the satellite instruments.

Considering the statistics parameters when the comparison of SB and GB UVI data is restricted to common dates, we observe that, for AS conditions, absolute bias and regression line slope are slightly worse for GOME-2 than for OMI at all sites, while relative bias and correlation coefficient are similar for both satellite instruments. For CS conditions, the three sites give different results. Indeed, in terms of absolute bias OMI UVI agree with GB data slightly better than GOME-2 UVI at VDA, OMI and GOME-2 UVI products compare with GB data equally at OHP, while at SDR site GOME-2 UVI agree with GB data slightly better than OMI UVI. In terms of median relative bias OMI and GOME-2 data agree with GB data equally at VDA, while it is slightly better at OHP and SDR for GOME-2. This later behaviour means that the absence of clouds at noon (CS conditions) is slightly better forecast by GOME-2 via COD estimates in the morning and in the afternoon. Though, the differences are subtle and globally the algorithms work equally well.

Such positive biases as obtained in this work, which for OMI-v1.3 are in agreement with other studies (Muyimbwa et al., 2015, Bernhard et al., 2015), might be partly explained by the satellite total ozone column underestimate, as shown in the modelling study of the present work. Though, further studies are still needed to understand and reduce the remaining existing biases between satellite-based and ground-based surface UVI at the three sites. OMI-v1.3 off-line correction uses a climatology for aerosol optical properties, so a reduction of the OMI bias might be obtained via a better characterisation of these aerosol properties, for example from simultaneous measurements. This recommendation is worth considering also for GOME-2. For GOME-2, the role of sub-pixel inhomogeneity could be investigated with respect to aerosol and cloud spatial variability, similar to what has been done for OMI (Weihs et al., 2008, Kazadzis et al., 2009b).

Finally the UVI estimates derived from satellite sensors OMI and GOME-2 are only weakly biased high (on average less than 0.5 unit of UVI at VDA and OHP and less that 1. at SDR), which, as mentioned above, is less risky for public health than a low bias, and thus OMI and GOME-2 noon-UVI datasets are quite reliable and can be used by the public.

Team list

Antti.Arola@fmi.fi; Frederique.Auriol@univ-lille1.fr; colette.brogniez@univ-lille1.fr; maxime.catalfamo@univ-lille1.fr; pierre.daconceicao@osupytheas.fr; christine.deroo@univ-lille1.fr; Niilo.Kalakoski@fmi.fi; Jukka.Kujanpaa@fmi.fi; jean-marc.metzger@univ-reunion.fr ;mikko.pitkanen@fmi.fi;work.beatrice.sauvage@gmail.com; guy.tournois@osupytheas.fr;

Copyright statement

Code availability

Data availability: Spectroradiometer measurements are currently available at http://www-loa.univ-lille1.fr/index.php/observation/sites.html and at ftp://ftp.cpc.ncep.noaa.gov/ndacc/station/

OMI data are available at http://avdc.gsfc.nasa.gov/index.php?site=595385375&id=79. GOME-2 data are available at http://o3msaf.fmi.fi/offline_access.html.

Appendix: Statistics definitions for n pairs of UVI data

Difference: $diff_i = SB_i - GB_i$

Mean Bias (mean difference): $mBias = \frac{1}{n}\sum_{i=1}^{n} diff_i$

Root-Mean-Square difference: $RMS = \sqrt{\frac{1}{n-1}\sum_{i=1}^{n}(diff_i)^2}$

Relative difference in %: $rdiff_i = 100.\times\frac{SB_i - GB_i}{GB_i}$

Mean Relative Bias (mean relative difference) in %: $mrBias = \frac{1}{n}\sum_{i=1}^{n} rdiff_i$

Root-Mean-Square relative difference: $rRMS = \sqrt{\frac{1}{n-1}\sum_{i=1}^{n}(rdiff_i)^2}$

A RMS (rRMs) close to mBias (mrBias) means that the differences (relative differences) are mostly positive

Standard deviation of the relative differences (dispersion around the mean): $STD = \sqrt{\frac{1}{n-1}\sum_{i=1}^{n}(rdiff_i - mrBias)^2}$

Since differences and relative differences distributions are skewed the following parameter are also used:

Median: mid-value of the differences (in UVI) or of the relative differences (in %)

p_{10}, p_{90}: the relative difference value at the 10^{th} and 90^{th}-percentile

675

Author Contributions

C.B. and F.A. oversaw the measurements. C.B. prepared the manuscript with contributions from A.A., J.K., F.A., M.R.A.P. and N.K.. The instruments were operated by F.A., M.C., J.M.M., G.T. and P.D.C.. C.D. contributed to collecting data and processing them. C. B., A. A., J. K., M.R.A.P., N. K. and B. S. contributed to the analysis of the results.

680

Acknowledgements

C.B. thanks L. Labonnote (LOA) for helpful discussions and R. De Filippi for automation of data transfer. P. Goloub and T. Podvin are acknowledged for their help in selecting the AERONET/PHOTONS data. The sites are supported by CNES within the French program TOSCA. SDR site is also supported by "la région La Réunion". Development of the OUV product has been partly funded by EUMETSAT.

685

References

Antón, M., and Loyola, D.: Influence of cloud properties on satellite total ozone observations, J. Geophys. Res., vol. 116, D03208, doi:10.1029/2010JD014780, 2011.

690

Antón, M., Piedehierro, A.A., Alados-Arboledas, L., Wolfran, E., and Olmo, F.J.: Extreme ultraviolet index due to broken clouds at a midlatitude site, Granada (southeastern Spain), Atmospheric Environment, vol. 118, p. 10-14, 2012.

Arola, A., Kazadzis, S., Lindfors, A., Krotkov, N., Kujanpää, J., Tamminen, J., Bais, A., di Sarra, A., Villaplana, J. M., Brogniez, C., Siani, A. M., Janouch, M., Weihs, P., Webb, A., Koskela, T., Kouremeti, N., Meloni, D., Buchard, V.,

695

Auriol, F., Ialongo, I., Staneck, M., Simic, S., Smedle, A., and Kinne, S.: A new approach to correct for absorbing aerosols in OMI UV, J. Geophys. Res., vol. 36, L22805, doi: 10.1029/2009GL041137, 2009.

Bernhard, G., Arola, A., Dahlback, A., Fioletov, V., Heikkilä, A, Johnsen, B., Koskela, T., Lakkala, K., Svendby, T., and Tamminen, J.: Comparison of OMI UV observations with ground-based measurements at high northern latitudes, www.atmos-chem-phys.net/15/7391/2015/ doi:10.5194/acp-15-7391, 2015.

700

Bernhard., G., and Seckmeyer, G.: Uncertainty of measurements of spectral solar UV irradiance, J. Geophys. Res., vol. 104, 14321–14345, 1999.

Buchard, V., Brogniez, C., Auriol, F., Bonnel, B., Lenoble, J., Tanskanen, A., Bojkov B., and Veefkind, P.: Comparison of OMI ozone and UV irradiance data with ground-based measurements at two French sites, Atmos. Chem. Phys., vol. 8, p. 4517-4528, 2008.

Buntoung, S., and Webb, A.R.: Comparison of erythemal UV irradiances from Ozone Monitoring Instrument (OMI) and ground-based data at four Thai stations, J. Geophys. Res., 115, D18215, doi:10.1029/2009JD013567, 2010.

Diffey, B., and McKinlay, A. F.: A reference action spectrum for ultraviolet induced erythema in human skin, Human Exposure to UV radiation: Risks and Regulations, 83-87, Elsevier, NY, 1987.

Dobber, M., Voors, R., Dirksen, R., Kleipool, Q., Levelt, P.: The High-Resolution Solar Reference Spectrum between 250 and 550 nm and its Application to Measurements with the Ozone Monitoring Instrument, Solar Phys , 249: 281–291 DOI 10.1007/s11207-008-9187-7, 2008.

Feister, U. and Grewe, R.: Spectral albedo measurements in the UV and visible region over different types of surfaces, Photochem. Photobiol., 62, 736–744, 1995.

GOME-2 Product guide, EUMETSAT, 2011.

Gröbner, J., Schreder, J., Kazadzis, S., Bais, A. F., Blumthaler, M., Görts, P., Tax, R., Koskela, T., Seckmeyer, G., Webb, A. R., and Rembges, D.: Traveling reference spectroradiometer for routine quality assurance of spectral solar ultraviolet irradiance measurements, Appl. Opt., doi: 10.1364/AO.44.005321, 2005.

Holben, B. N., Eck, T. F., Slutsker, I., Tanré, D., Buis, J. P., Setzer, A., Vermote, E., Reagan, J. A., Kaufman, Y. J., Nakajima, T., Lavenu, F., Jankowiak, I., and Smirnov, A.: AERONET – A federated instrument network and data archive for aerosol characterization, Remote Sens. Environ., 66, 1–6, 1998.

Houët, M.: Spectroradiométrie du rayonnement Solaire UV au sol: Améliorations apportées à l'instrumentation et au traitement des mesures. Analyse pour l'évaluation du contenu atmosphérique en ozone et en aérosols, Ph.D. thesis, Univ. of Lille, France, 2003.

Houët, M., and Brogniez, C.: Ozone column retrieval from solar UV irradiance measurements at ground level: Sensitivity tests and uncertainty estimation, J. Geophys. Res., 109, D15302, doi:10.1029/2004JD004703, 2004.

Ialongo, I., Casale, G. R., and Siani, A. M.: Comparison of total ozone and erythemal UV data from OMI with ground-based measurements at Rome station, Atmos. Chem. Phys., 8, 3283– 3289, 2008.

Kalakoski, N.: O3M SAF Validation Report, Offline UV Index, SAF/O3M/FMI/VR/OUV/091, FMI, http://o3msaf.fmi.fi/docs/vr/Validation_Report_OUV_Feb_2009.pdf, 2009.

Kazadzis, S., Bais, A., Arola, A., Krotkov, N., Kouremeti, N., and Meleti, C.: Ozone Monitoring Instrument spectral UV irradiance products: comparison with ground based measurements at an urban environment, Atmos. Chem. and Phys., vol. 9, p. 585-594, 2009a.

Kazadzis, S., Bais, A., Balis, D., Kouremeti, N., Zempila, M., Arola, A., Giannakaki, E., Amiridis, V., and Kazantzidis, A.: Spatial and temporal UV irradiance and aerosol variability within the area of an OMI satellite pixel, Atmos. Chem. and Phys., vol. 9, p. 4593-4601, 2009b.

Kinne, S.: Towards an observation-tied AOD climatology, presentation in AT2 Aerosol Workshop, Bremen, June 2007.

Kinne, S., O'Donnel, D., Stier, P., Kloster, S., Zhang, K., Schmidt, H., Rast, S., Giorgetta, M., Eck, T. F., and Stevens, B. : MAC-v1: A new global aerosol climatology for climate studies, J. Adv. Model. Earth Syst., 5, 704–740, doi:10.1002/jame.20035, 2013.

Köpke, P., M. Hess, I. Schult, and E.P. Shettle: Global Aerosol Data Set, Report No. 243, Max-Planck-Institut für Meteorologie, Hamburg, ISSN 0937-1060, 1997.

Krotkov, N.A., Herman, J., Bhartia, P.K., Seftor, C., Arola, A., Kaurola, J., Taalas, P., and Vasilkov, A.: OMI Surface UV Irradiance Algorithm, in OMI Algorithm Theoretical Basis Document, Volume III: Clouds, Aerosols, and Surface UV Irradiance, ATBD-OMI-03, http://eospso.gsfc.nasa.gov/eos_homepage/for_scientists/atbd/docs/OMI/ATBD-OMI-03.pdf, 2002.

Kujanpää, J., Algorithm Theoretical Basis Document, Offline UV (OUV) Products, SAF/O3M/FMI/ATBD/001,FMI, http://o3msaf.fmi.fi/docs/atbd/Algorithm_Theoretical_Basis_Document_OUV_Jun_2013.pdf, 2013.

Kujanpää, J., and Kalakoski, N.: Operational surface UV radiation product from GOME-2 and AVHRR/3 data, Atmos. Meas. Tech., 8, 4399–4414, doi:10.5194/amt-8-4399-2015, 2015.

Levelt, P.F., van den Oord, G.H.J., Dobber, M.R., Mälkki, A., Visser, H., de Vries, J., Stammes, P., Lundell, J. O. V., and Saari, H.: The Ozone Monitoring Instrument, IEEE Transactions on Geoscience and Remote Sensing, vol. 44, no. 5, p. 1093-1101, 2006.

McKenzie, R. L., Johnston, P. V., Smale, D., Bodhaine, B. A., and Madronich, S.: Altitude effects on UV spectral irradiance deduced from measurements at Lauder, New Zealand, and at Mauna Loa Observatory, Hawaii, J. Geophys. Res., vol. 106, 22845-22860, 2001.

Munro, R., Lang, R., Klaes, D., Poli, G., Retscher, C., Lindstrot, R., Huckle, R., Lacan, A., Grzegorski, M., Holdak, A., Kokhanovsky, A., Livschitz, J., and Eisinger, M.: The GOME-2 instrument on the Metop series of satellites: instrument design, calibration, and level 1 data processing – an overview, Atmos. Meas. Tech. Discuss., 8, 8645–8700, 2015.

Muyimbwa, D., Dahlback, A., Ssenyonga, T., Chen, Y.-C., Stamnes, J. J., Frette, Ø. , and Hamre, B.: Validation of ozone monitoring instrument ultraviolet index against ground-based UV index in Kampala, Uganda, Appl. Opt., doi.org/10.1364/AO.54.008537, 2015.

Paur, R. J., and Bass A. : The ultraviolet cross sections of ozone: II. Results and temperature dependence, in Atmospheric Ozone, Proceedings of the Quadrennial Ozone Symposium, Halkidiki, Greece, edited by C. Zeferos and A. Ghazi, pp. 611–616, D. Reidel, Norwell, Mass., 1985.

Stamnes, K., Tsay, S.-C., Wiscombe, W., and Jayaweera, K.: Numerically stable algorithm for discrete-ordinatemethod radiative transfer in multiple scattering and emitting layered media, Appl. Optics, 27, 2502–2509, 1988.

Tanskanen, A.: Lambertian surface albedo climatology at 360 nm from TOMS data using moving time-window technique, Proc. XX Quadrennial Ozone Symposium, June 2004.

Tanskanen, A., Lindfors, A., Määttä, A., Krotkov, N., Herman, J., Kaurola, J., Koskela, T., Lakkala, K., Fioletov, V., Bernhard, G., McKenzie, R., Kondo, Y., O'Neill, M., Slaper, H., den Outer, P., Bais, A. F., and Tamminen, J.: Validation of daily erythemal doses from Ozone Monitoring Instrument with ground-based UV measurement data, J. Geophys. Res., vol. 112, D24S44, doi: 10.1029/2007JD008830, 2007.

Van Weele, M., Martin, J., Blumthaler, M., Brogniez, C., Den Outer, P. N., Engelsen, O., Lenoble, J., Mayer, B., Pfister, G., Ruggaber, A., Walravens, B., Weihs, P., Gardiner, B. G., Gillotay, D., Haferl, D., Kylling, A., Seckmeyer, G., and Wauben, W. M. F.: From model intercomparison toward benchmark UV spectra for six real atmospheric cases, J. Geophys. Res. 105(D4), 4915-4925, 2000.

Weihs, P., Blumthaler, M., Rieder, H.E., Kreuter, A., Simic, S., Laube, W., Schmalwieser, A.W., Wagner, J.E., and Tanskanen, A.: Measurements of UV irradiance within the area of one satellite pixel, Atmos. Chem. and Phys., vol. 8, p. 5615–5626, 2008.

York, D., Evensen, N. M., López Martínez, M., and De Basabe Delgado, J.: Unified equations for the slope, intercept, and standard errors of the best straight line, American Journal of Physics 72, 367; doi: 10.1119/1.1632486, 2004.

	n	Mean bias UVI	Median bias UVI	RMS UVI	Mean rel bias %	Median rel bias %	rRMS %	p_{10}	p_{90}	Slope (unc.)	Interc. UVI	r
VDA												
OMI-V1.2-SPECTRO	1356	0.57	0.38	0.94	31.5	20.9	54.8	-7.8	84.9	1.17 (0.01)	-0.01	0.95
OMI-V1.3-SPECTRO	1346	0.32	0.21	0.70	22.5	12.5	46.8	-14.9	71.4	1.08 (0.01)	0.00	0.95
GOME-2-SPECTRO	795	0.50	0.33	0.90	20.6	12.1	45.0	-16.8	64.3	1.12 (0.01)	-0.12	0.94
OHP												
OMI-V1.2-SPECTRO	1313	0.91	0.83	1.29	31.3	19.7	57.2	1.7	72.4	1.14 (0.01)	0.07	0.96
OMI-V1.3-SPECTRO	1283	0.42	0.32	0.89	21.6	9.3	54.6	-8.0	57.4	1.04 (0.01)	0.09	0.96
GOME-2-SPECTRO	1041	0.53	0.41	0.97	19.8	8.4	51.6	-11.9	60.3	1.05 (0.01)	-0.03	0.96
SDR												
OMI-V1.2-SPECTRO	782	1.30	0.80	2.71	27.9	10.7	62.8	-12.5	80.9	0.86 (0.02)	1.61	0.72
OMI-V1.3-SPECTRO	774	1.39	0.78	2.70	29.0	10.4	64.2	-9.2	85.9	0.91 (0.02)	1.36	0.74
GOME-2-SPECTRO	642	1.56	0.87	2.81	34.6	10.8	75.3	-6.0	99.9	0.78 (0.03)	2.45	0.71

Table 1. Summary of UVI OMI-GOME-2 validation results at the three sites for distances (Dist) between the station and the CTP/grid cell center point ≤100 km and for all-sky conditions. Results for the two OMI versions are presented. n is the number of points, r is the correlation coefficient. We have indicated the slope (uncertainty in parentheses) and intercept (interc.) of the regression line. See the statistics definitions in Appendix.

	n	Mean bias UVI	Median bias UVI	RMS UVI	Mean rel bias %	Median rel bias %	rRMS %	p_{10}	p_{90}	Slope (unc.)	Interc. UVI	r
VDA												
OMI-V1.2-SPECTRO	72	0.71	0.79	0.84	16.8	18.1	17.8	10.0	23.3	1.20 (0.01)	-0.08	1.00
OMI-V1.3-SPECTRO	72	0.32	0.32	0.40	7.9	8.4	10.2	0.0	15.5	1.10 (0.01)	-0.06	1.00
GOME-2-SPECTRO	37	0.33	0.39	0.48	5.2	8.3	11.1	-9.8	12.7	1.14 (0.02)	-0.31	0.99
OHP												
OMI-V1.2-SPECTRO	266	0.88	0.90	1.03	16.3	17.2	17.4	9.2	22.7	1.18 (0.01)	-0.05	1.00
OMI-V1.3-SPECTRO	263	0.26	0.24	0.42	5.5	5.8	8.9	-0.7	12.1	1.05 (0.01)	0.01	0.99
GOME-2-SPECTRO	200	0.24	0.25	0.46	1.8	4.1	9.4	-11.6	11.6	1.09 (0.01)	-0.27	0.99
SDR												
OMI-V1.2-SPECTRO	175	0.29	0.44	1.10	3.6	5.0	11.2	-9.9	14.8	1.02 (0.03)	0.01	0.94
OMI-V1.3-SPECTRO	170	0.30	0.37	0.87	3.5	4.2	9.4	-7.9	13.7	1.03 (0.02)	0.00	0.96
GOME-2-SPECTRO	145	0.18	0.30	0.80	2.5	3.8	8.1	-8.1	10.6	0.98 (0.02)	0.26	0.96

Table 2. Same as Table 1 but for CS conditions.

	n	Mean bias UVI	Median bias UVI	RMS UVI	Mean rel bias %	Median rel bias %	rRMS %	p_{10}	p_{90}	Slope (unc.)	Interc. UVI	r
VDA												
Dist OMI-V1.3-SPECTRO	349	0.25	0.16	0.61	15.4	10.3	34.8	-15.4	50.0	1.06 (0.02)	-0.01	0.96
Dist GOME-2-SPECTRO	114	0.43	0.28	0.79	15.8	14.3	31.0	-13.7	52.4	1.10 (0.03)	-0.05	0.95
OHP												
Dist OMI-V1.3-SPECTRO	273	0.42	0.34	0.76	19.2	8.3	46.2	-3.2	44.8	1.05 (0.02)	0.06	0.97
Alti OMI-V1.3-SPECTRO	687	0.42	0.32	0.78	21.9	9.3	54.7	-6.0	53.2	1.05 (0.01)	0.07	0.97
Dist GOME-2-SPECTRO	144	0.60	0.49	1.12	22.2	10.3	54.3	-14.0	59.7	0.99 (0.03)	0.09	0.95
SDR												
Dist OMI-V1.3-SPECTRO	341	1.06	0.60	2.41	21.5	8.1	52.7	-12.6	67.1	0.91 (0.03)	1.10	0.75
Alti OMI-V1.3-SPECTRO	576	1.56	0.94	2.83	32.0	11.9	68.3	-6.4	93.5	0.92 (0.03)	1.45	0.74
Dist GOME-2-SPECTRO	93	1.73	1.00	3.17	40.2	11.0	91.5	-7.7	114.4	0.62 (0.09)	3.67	0.60

Table 3. Same as Table 1 but with a filter on the distance between the station and the CTP/grid cell center point (Dist≤10 km), and with a filter on OMI CTP_altitude.

At OHP the altitude filter is: Site_altitude - 250 m ≤ CTP_altitude ≤ Site_altitude + 250 m.

At SDR the altitude filter is: 0 m ≤ CTP_altitude ≤ Site_altitude + 250 m

	n	Mean bias UVI	Median bias UVI	RMS UVI	Mean rel bias %	Median rel bias %	rRMS %	p_{10}	p_{90}	Slope (unc.)	Interc. UVI	r
VDA												
Dist OMI-V1.3-SPECTRO	14	0.28	0.32	0.36	5.4	6.6	8.0	-2.8	9.5	1.09 (0.01)	-0.08	1.00
Dist GOME-2-SPECTRO	2											
OHP												
Dist OMI-V1.3-SPECTRO	53	0.29	0.25	0.41	5.2	5.3	8.6	-0.4	11.1	1.07 (0.02)	-0.09	0.99
Alti OMI-V1.3-SPECTRO	145	0.29	0.24	0.40	5.8	5.9	8.3	-0.4	12.0	1.05 (0.01)	0.00	1.00
Dist GOME-2-SPECTRO	19	0.23	0.18	0.53	0.3	4.5	11.0	-19.3	8.8	1.11 (0.03)	-0.33	0.99
SDR												
Dist OMI-V1.3-SPECTRO	89	0.13	0.28	0.89	1.8	3.8	9.4	-13.1	10.7	1.00 (0.04)	0.06	0.96
Alti OMI-V1.3-SPECTRO	119	0.41	0.45	0.82	4.7	5.5	9.1	-4.1	14.0	1.05 (0.03)	-0.06	0.98
Dist GOME-2-SPECTRO	16	0.01	0.23	0.89	1.3	3.2	8.0	-10.2	6.0	0.90 (0.07)	0.88	0.96

815

Table 4. Same as Table 3 but for CS conditions

820

	n	Mean bias UVI	Median bias UVI	RMS UVI	Mean el bias %	Median rel bias %	rRMS %	p_{10}	p_{90}	Slope (unc.)	Interc. UVI	r
VDA												
OMI-V1.3-SPECTRO	681	0.37	0.29	0.72	21.2	12.1	41.8	-10.6	65.5	1.05 (0.01)	0.08	0.95
GOME-2-SPECTRO	681	0.50	0.32	0.89	20.2	12.1	44.6	-16.9	64.9	1.12 (0.02)	-0.12	0.94
OHP												
OMI-V1.3-SPECTRO	821	0.39	0.30	0.83	20.5	8.5	51.9	-8.0	55.9	1.04 (0.01)	0.08	0.96
GOME-2-SPECTRO	821	0.54	0.43	0.97	19.1	8.4	50.6	-11.7	52.9	1.06 (0.01)	-0.06	0.96
SDR												
OMI-V1.3-SPECTRO	523	1.34	0.75	2.66	29.2	10.1	66.7	-10.4	81.2	0.91 (0.03)	1.28	0.74
GOME-2-SPECTRO	523	1.58	0.90	2.84	35.1	11.3	75.5	-6.4	104.1	0.78 (0.03)	2.40	0.70

Table 5. Same as Table 1 but for the same dates for both OMI and GOME-2.

825

	n	Mean bias UVI	Median bias UVI	RMS UVI	Mean el bias %	Median rel bias %	rRMS %	p_{10}	p_{90}	Slope (unc.)	Interc. UVI	r
VDA												
OMI-V1.3-SPECTRO	37	0.36	0.37	0.41	8.5	8.6	9.8	2.8	15.2	1.10 (0.01)	-0.07	1.00
GOME-2-SPECTRO	37	0.33	0.39	0.48	5.2	8.3	11.1	-9.8	12.7	1.14 (0.02)	-0.31	0.99
OHP												
OMI-V1.3-SPECTRO	168	0.27	0.23	0.38	5.5	5.4	8.6	-0.5	11.9	1.05 (0.01)	-0.01	0.99
GOME-2-SPECTRO	168	0.26	0.27	0.47	2.2	4.3	9.5	-11.4	11.6	1.09 (0.01)	-0.27	0.99
SDR												
OMI-V1.3-SPECTRO	115	0.29	0.35	0.91	3.6	4.3	9.8	-7.9	13.9	1.02 (0.03)	0.06	0.96
GOME-2-SPECTRO	115	0.14	0.24	0.84	2.2	3.4	8.4	-9.0	11.6	0.97 (0.03)	0.34	0.96

830 **Table 6**. Same as Table 2 but for the same dates for both OMI and GOME-2.

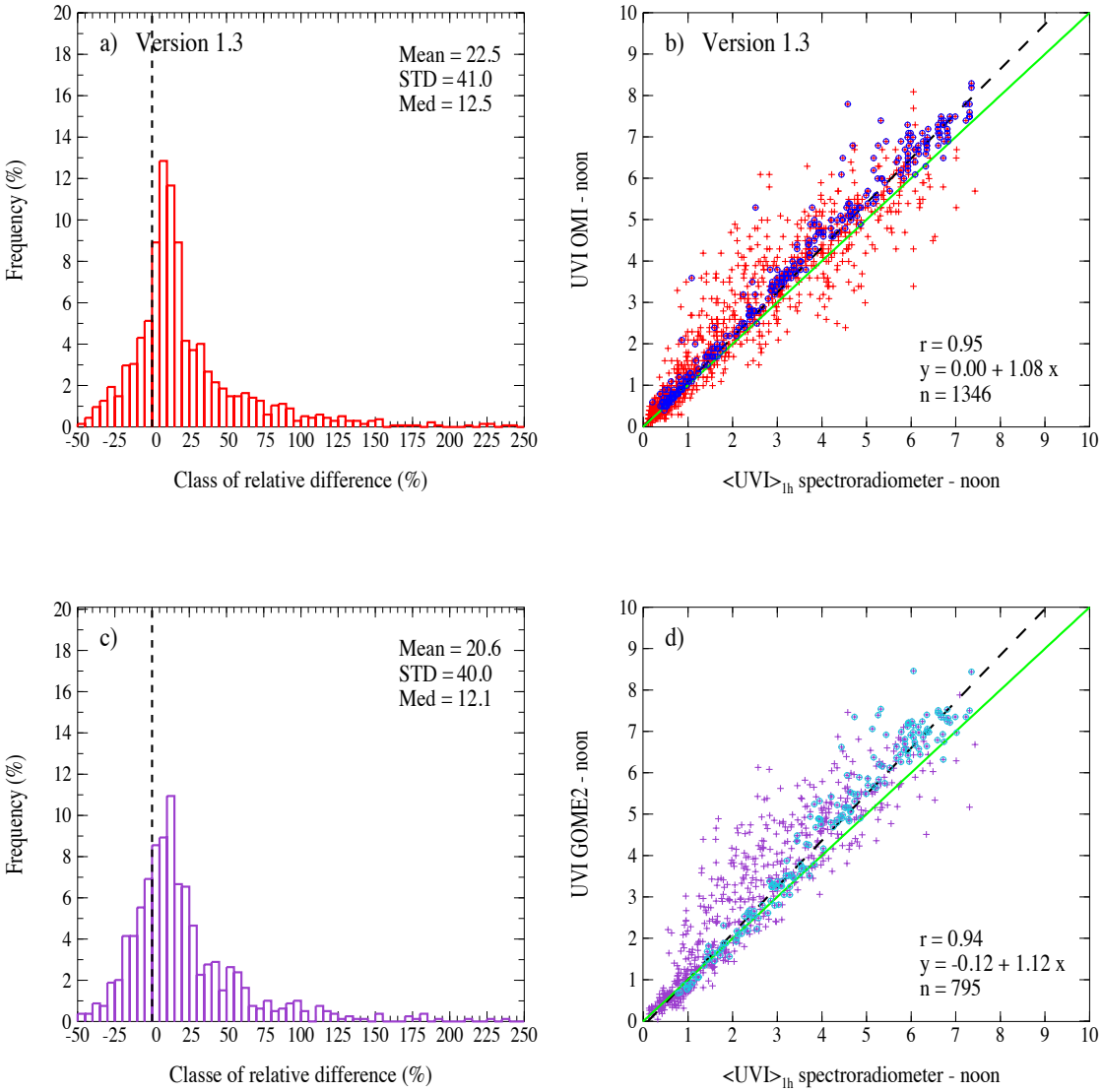

Figure 1. OMI-v1.3 (top panels) and GOME-2 (bottom panels) versus GB observations for Dist≤100 km and for AS conditions at VDA. GB measurements are averages over 1 h around local noon. a) and c): histograms of per cent relative difference (100.*(SB-GB)/GB) binned with 5 % interval. Few statistics parameters are indicated. b) and d): scatter plots of satellite estimates versus GB measurements. Circled crosses correspond to COD ≤ 1 (COD at overpass for OMI-v1.3, and at noon for GOME-2). The equation of the regression line (dash line) and the correlation coefficient are indicated. The green solid line is the first bisector. Percentiles for OMI: p_{10}=-14.9 %, p_{90}=71.4 %; for GOME-2: p_{10}=-16.8 %, p_{90}=64.3 %.

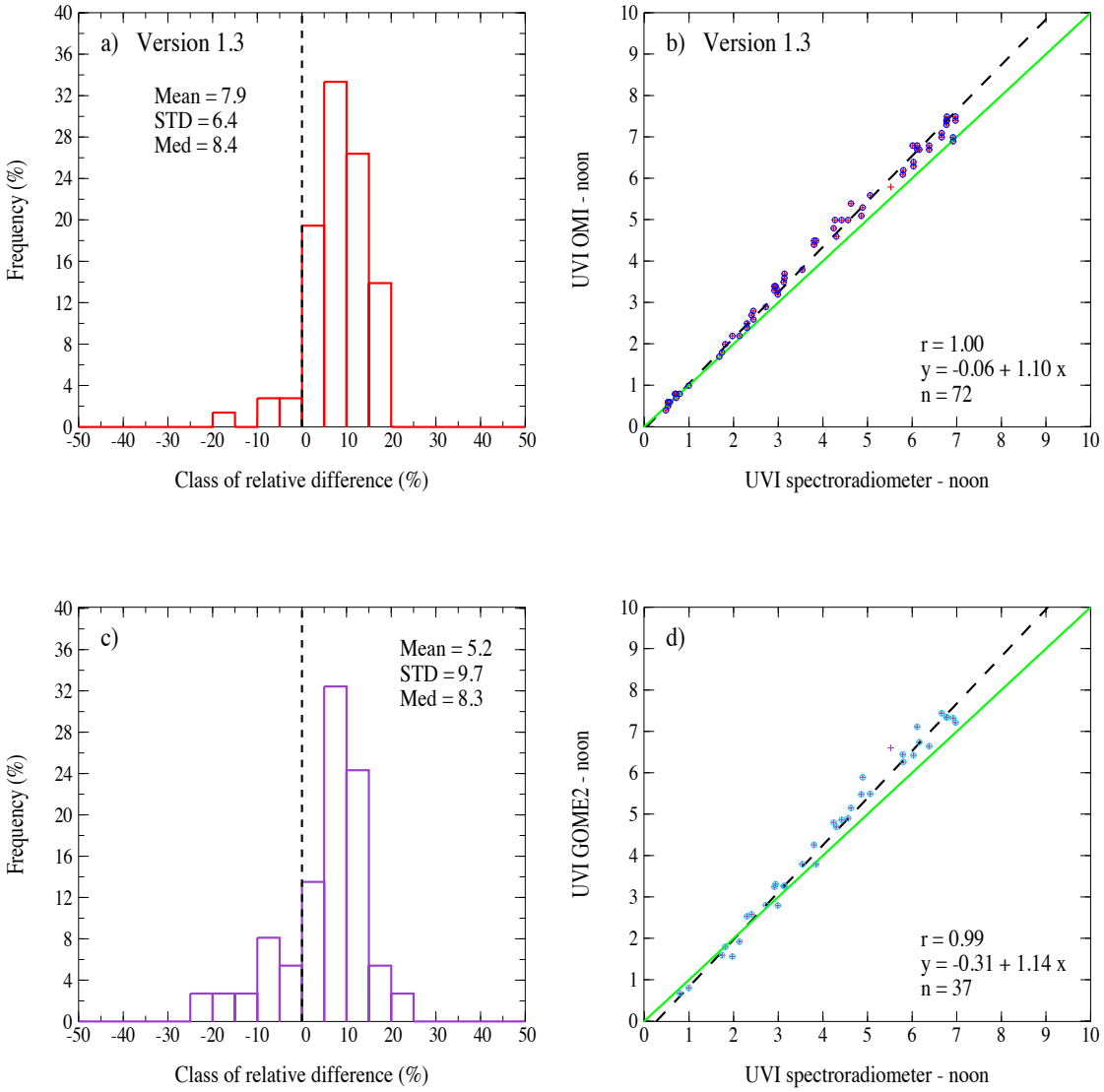

Figure 2. Same as Fig. 1 but for CS conditions at VDA. Percentiles for OMI: p_{10}=0.0 %, p_{90}=15.5 %; for GOME-2: p_{10}=-9.8 %, p_{90}=12.7 %.

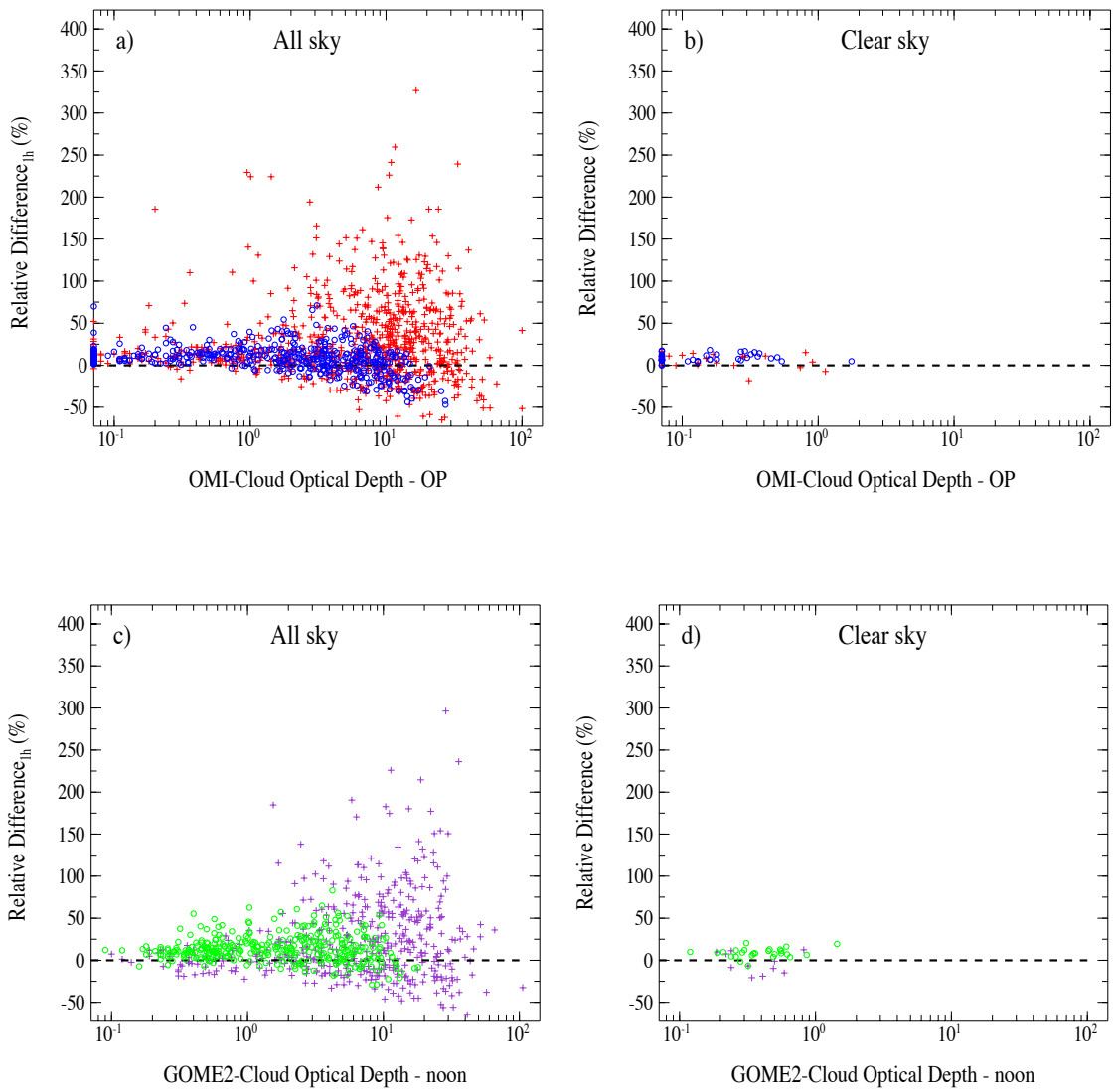

Figure 3. Per cent relative difference versus Cloud Optical Depth (COD) at VDA. COD is given at overpass for OMI-v1.3 (top panels), and at noon for GOME-2 (bottom panels). A filtering on the UVI value is made: blue and green circles correspond to UVI(GB value) ≥ 3. Left plots (a and c) for AS conditions, right plots (b and d) for CS conditions.

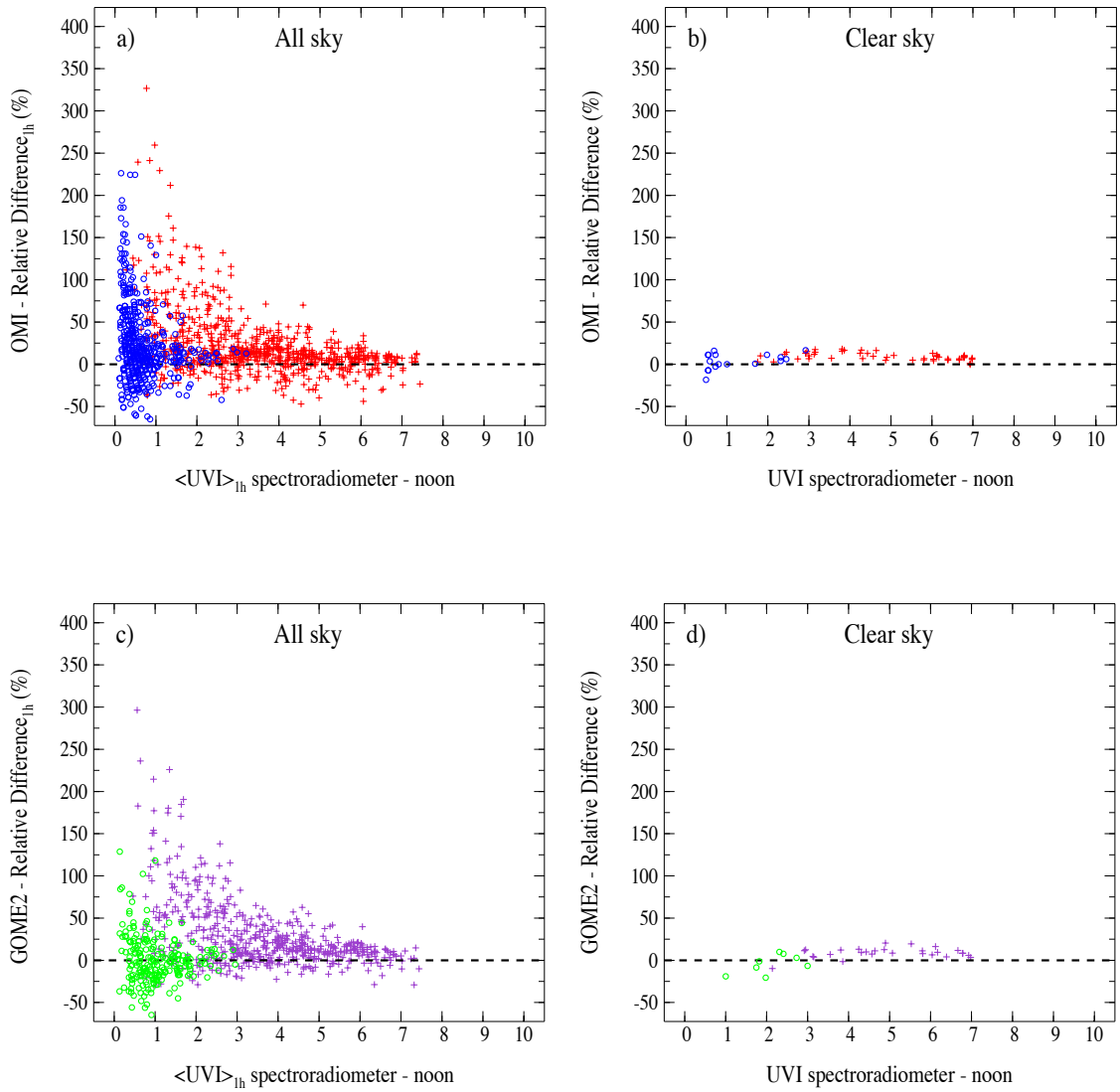

Figure 4. Per cent relative difference versus UVI from GB measurements at VDA for OMI-v1.3 (top panels) and GOME-2 (bottom panels). A filtering on SZA at overpass value is set: blue and green circles correspond to SZA > 60º. Left plots (a and c) for AS conditions, right plots (b and d) for CS conditions.

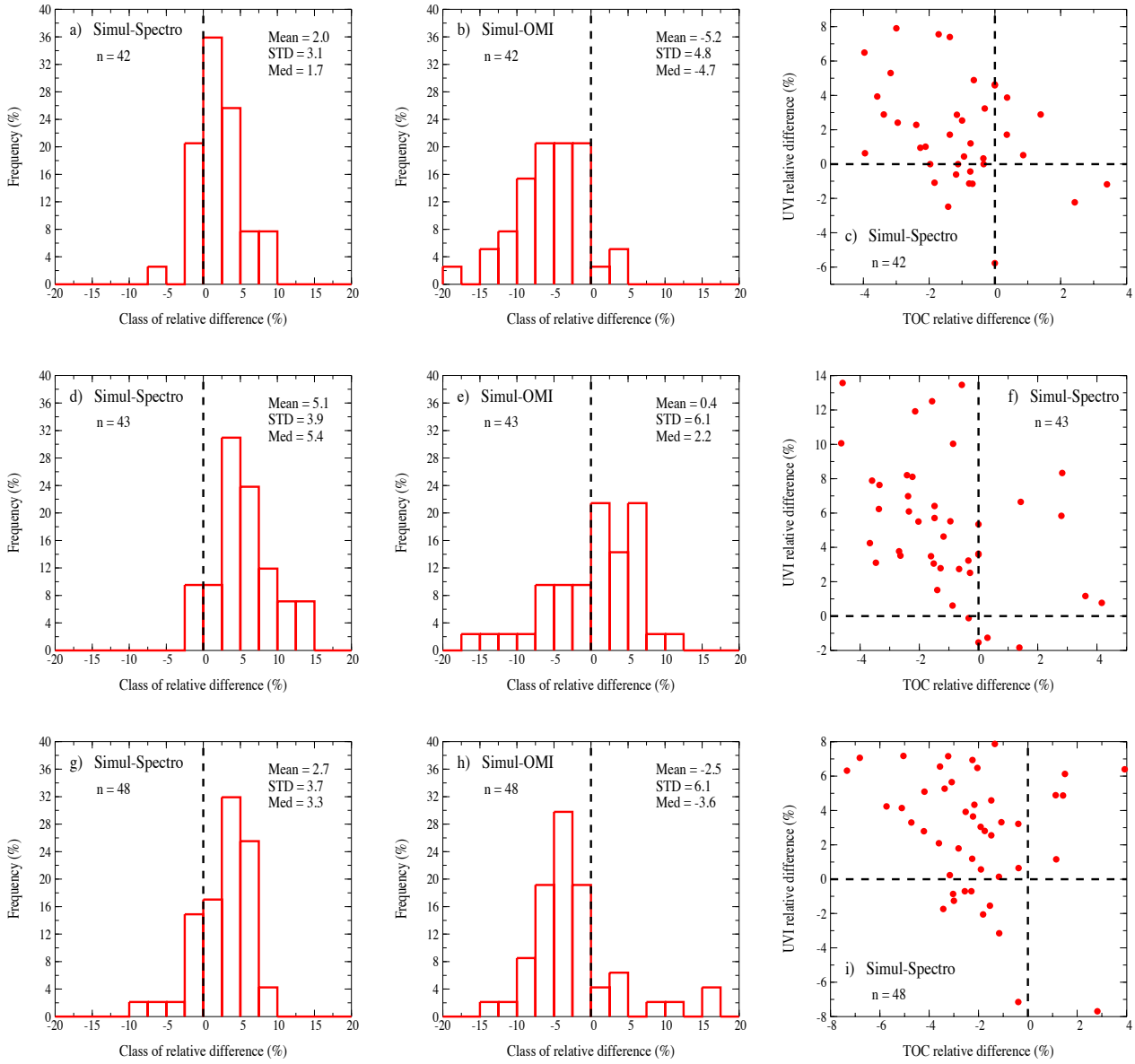

Figure 5. Histograms of the per cent relative difference between the simulated and the GB UVI (left panels), and between the simulated and the OMI UVI (middle panels). Relative difference in %: $rdiff_i = 200.\times\frac{SIMUL_i - MEAS_i}{SIMUL_i + MEAS_i}$. The right panels show the per cent relative difference between the simulated and the GB UVI versus the TOC relative difference (= $200.\times\frac{OMTO3_i - TOCspectro_i}{OMTO3_i + TOCspectro_i}$). Top panels (a,b,c) are for VDA, middle panels (d,e,f) for OHP, bottom panels (g,h,i) for SDR.

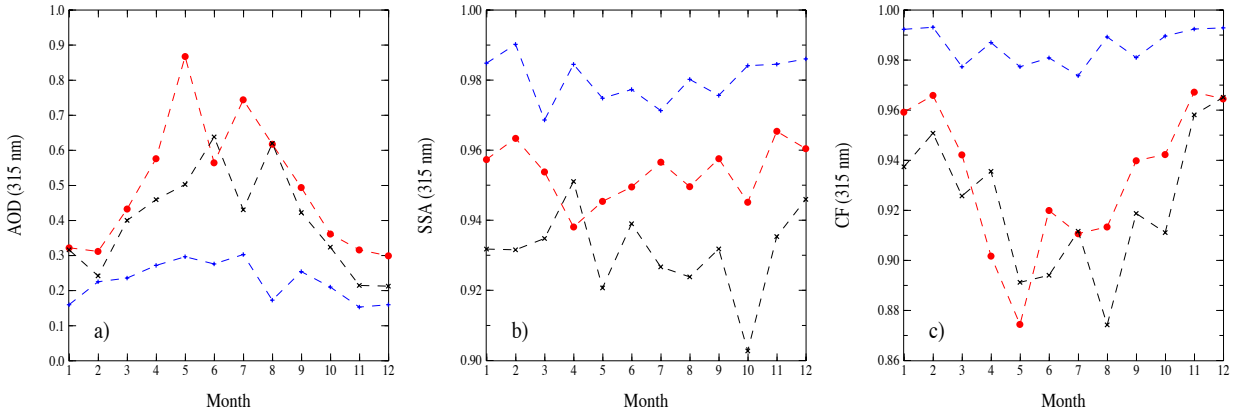

Figure 6. Aerosol data at 315 nm used in the OMI-v1.3 correction for absorbing aerosols. a) AOD ; b) SSA ; c) Correction factor. Red curves are for VDA site, black curves are for OHP and blue curves are for SDR.

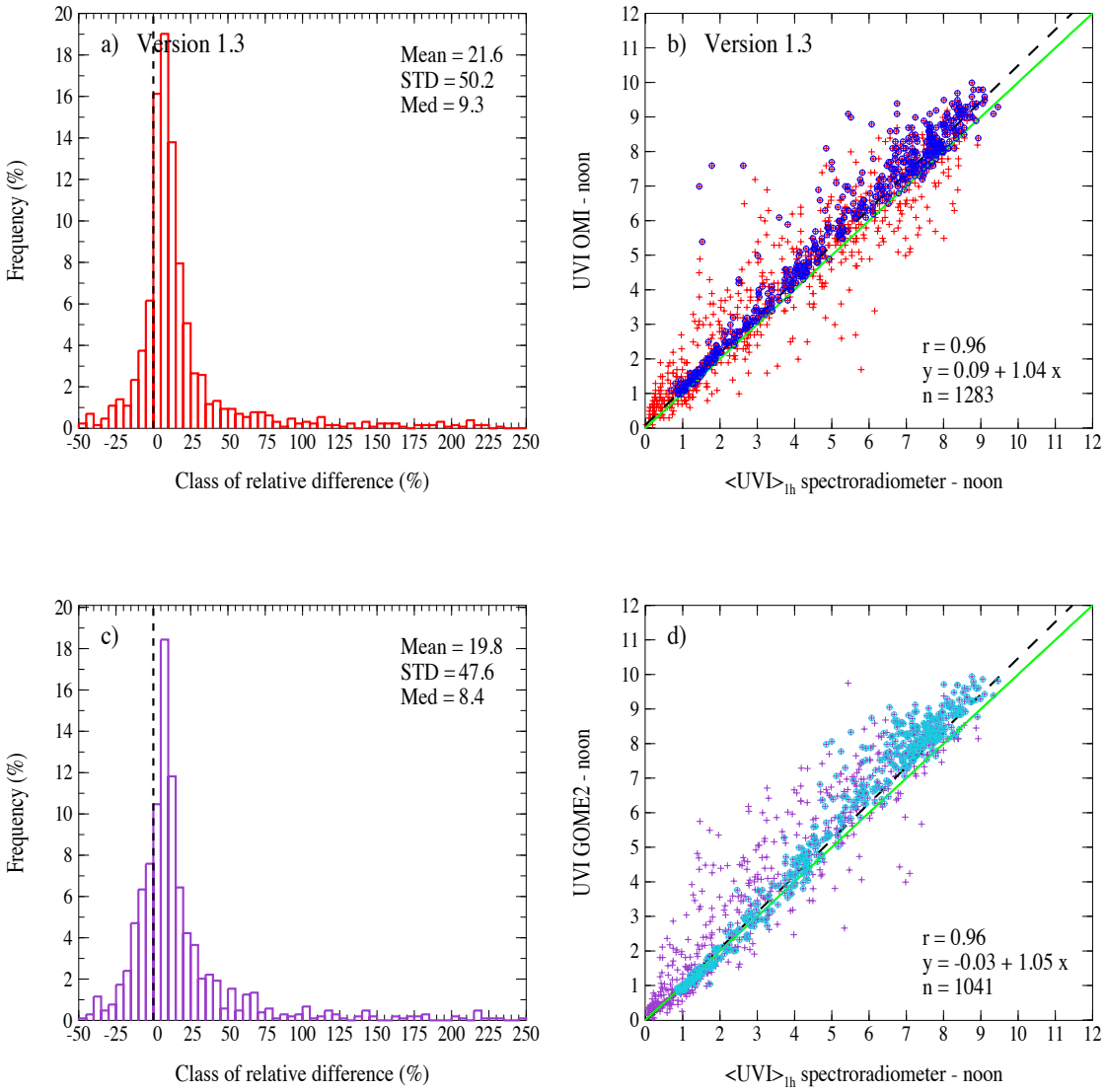

Figure 7. Same as Fig. 1 but for OHP. Percentiles for OMI: p_{10}=-8.0 %, p_{90}=57.4 %; for GOME-2: p_{10}=-11.9 %, p_{90}=60.3 %.

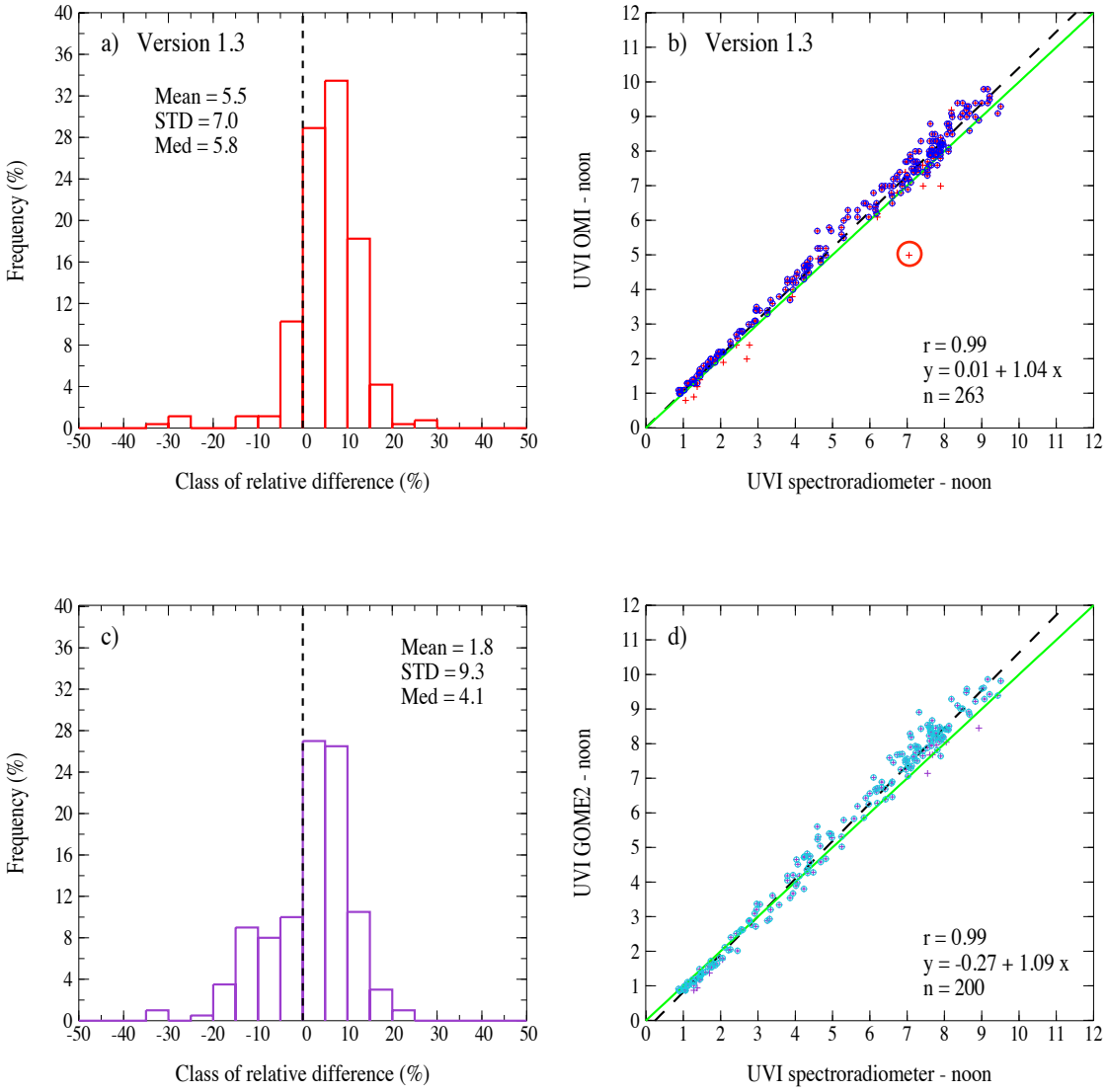

Figure 8. Same as Fig. 2 but for OHP. Percentiles for OMI: p_{10}=-0.7 %, p_{90}=12.1 %; for GOME-2: p_{10}=-11.6 %, p_{90}=11.6 %.

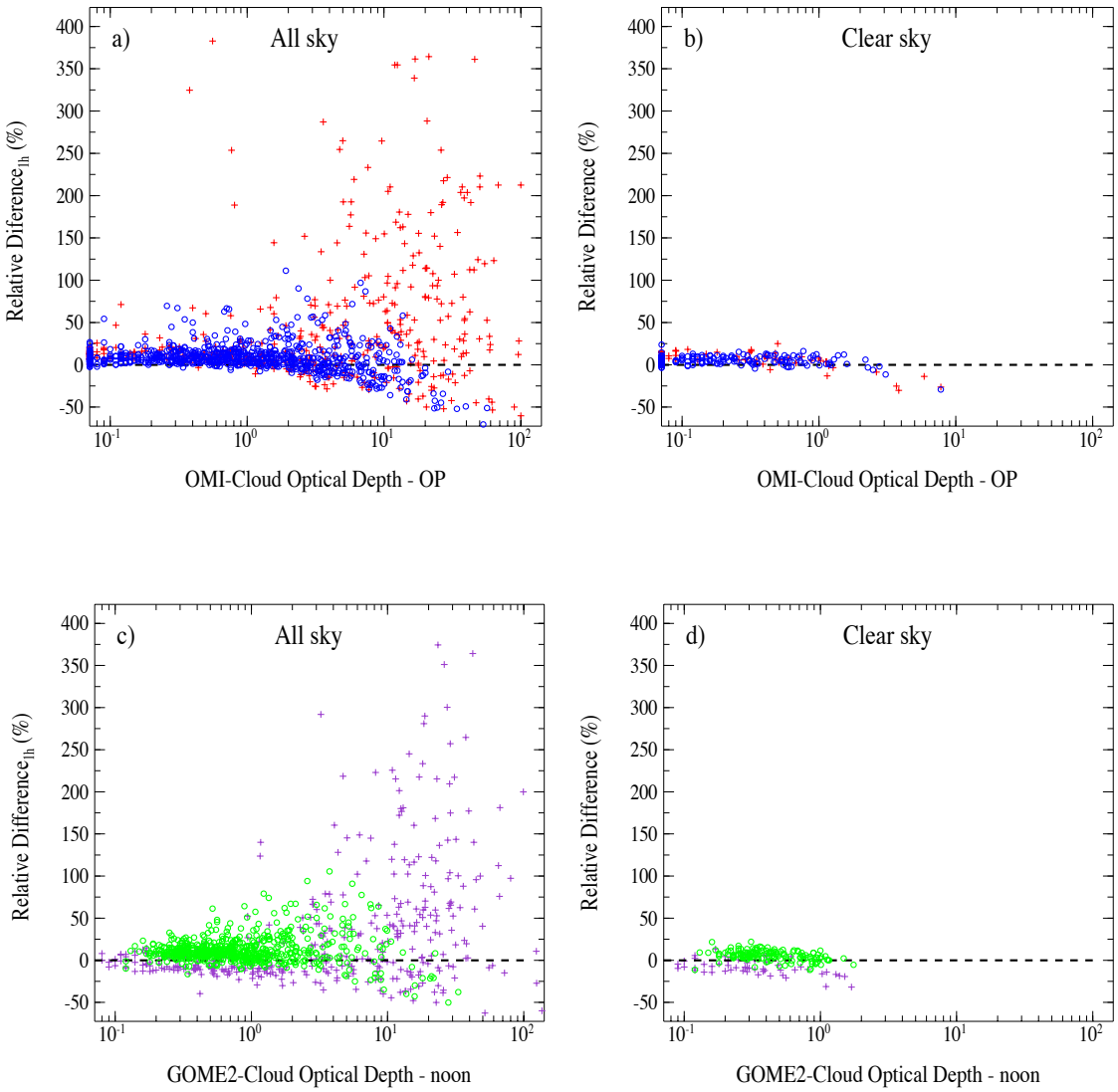

Figure 9. Same as Fig. 3 but for OHP.

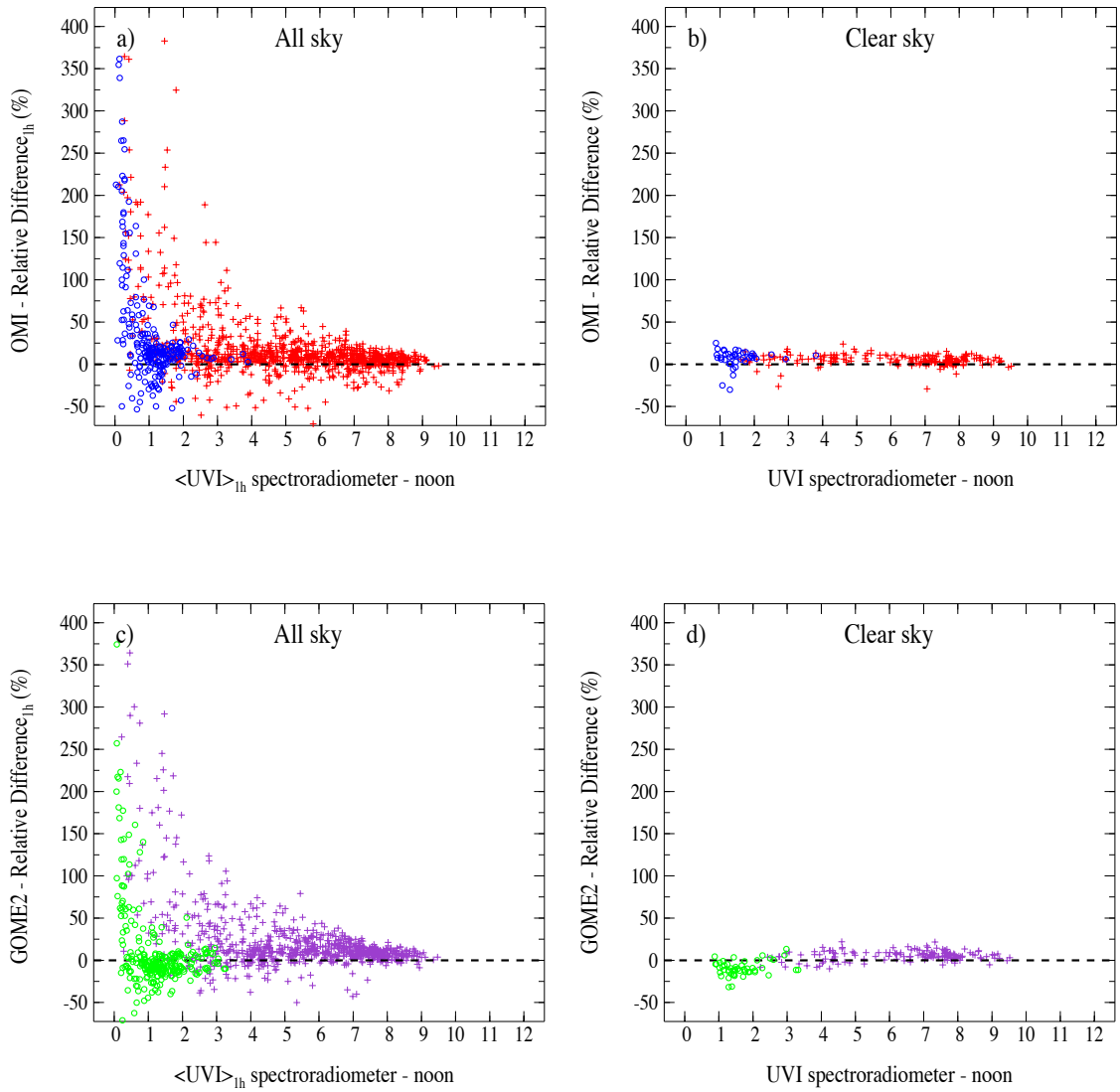

Figure 10. Same as Fig. 4 but for OHP.

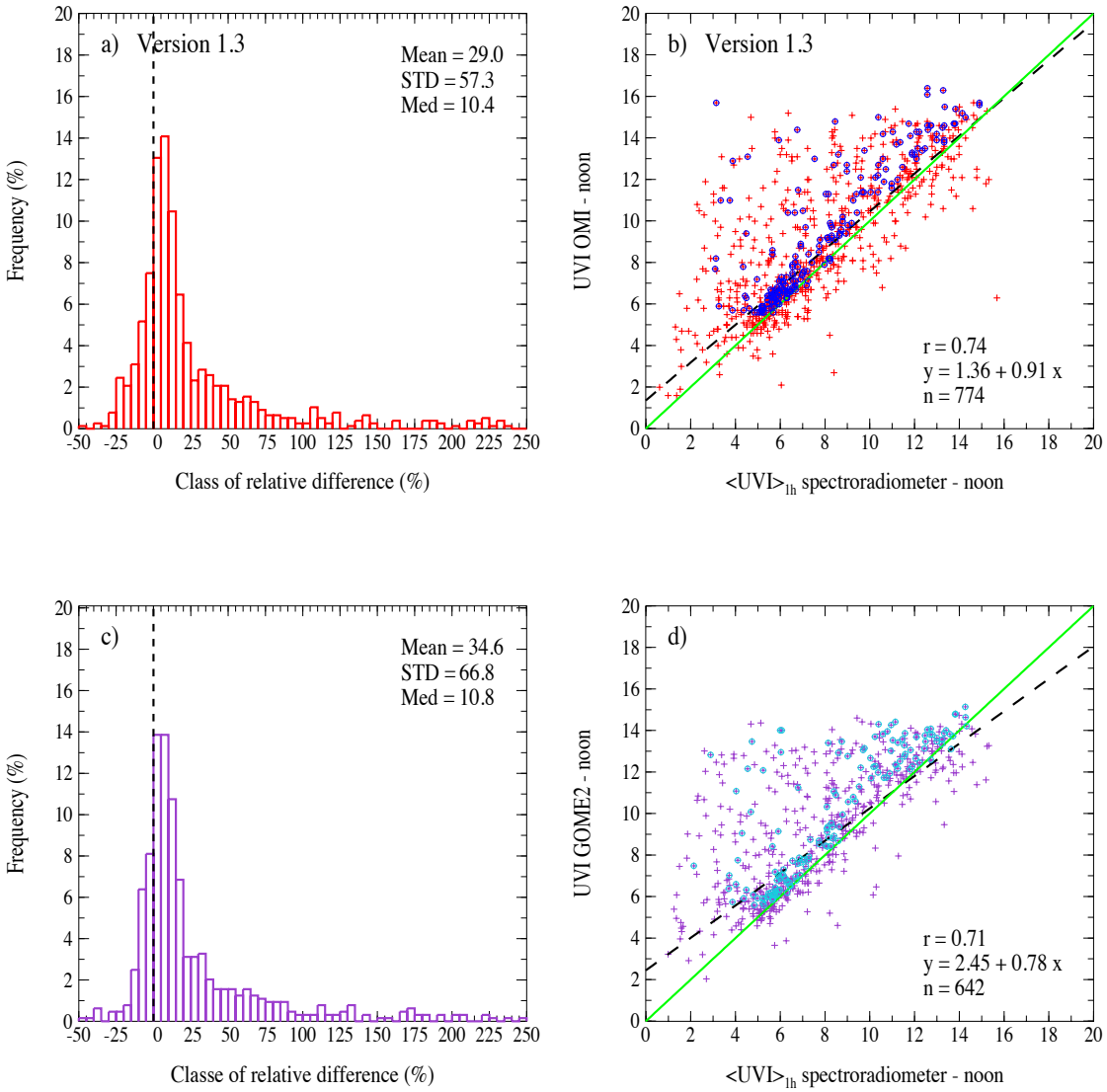

Figure 11. Same as Fig. 1 but for SDR. Percentiles for OMI: p_{10}=-9.2 %, p_{90}=85.9 %; for GOME-2: p_{10}=-6.0 %, p_{90}=99.9 %.

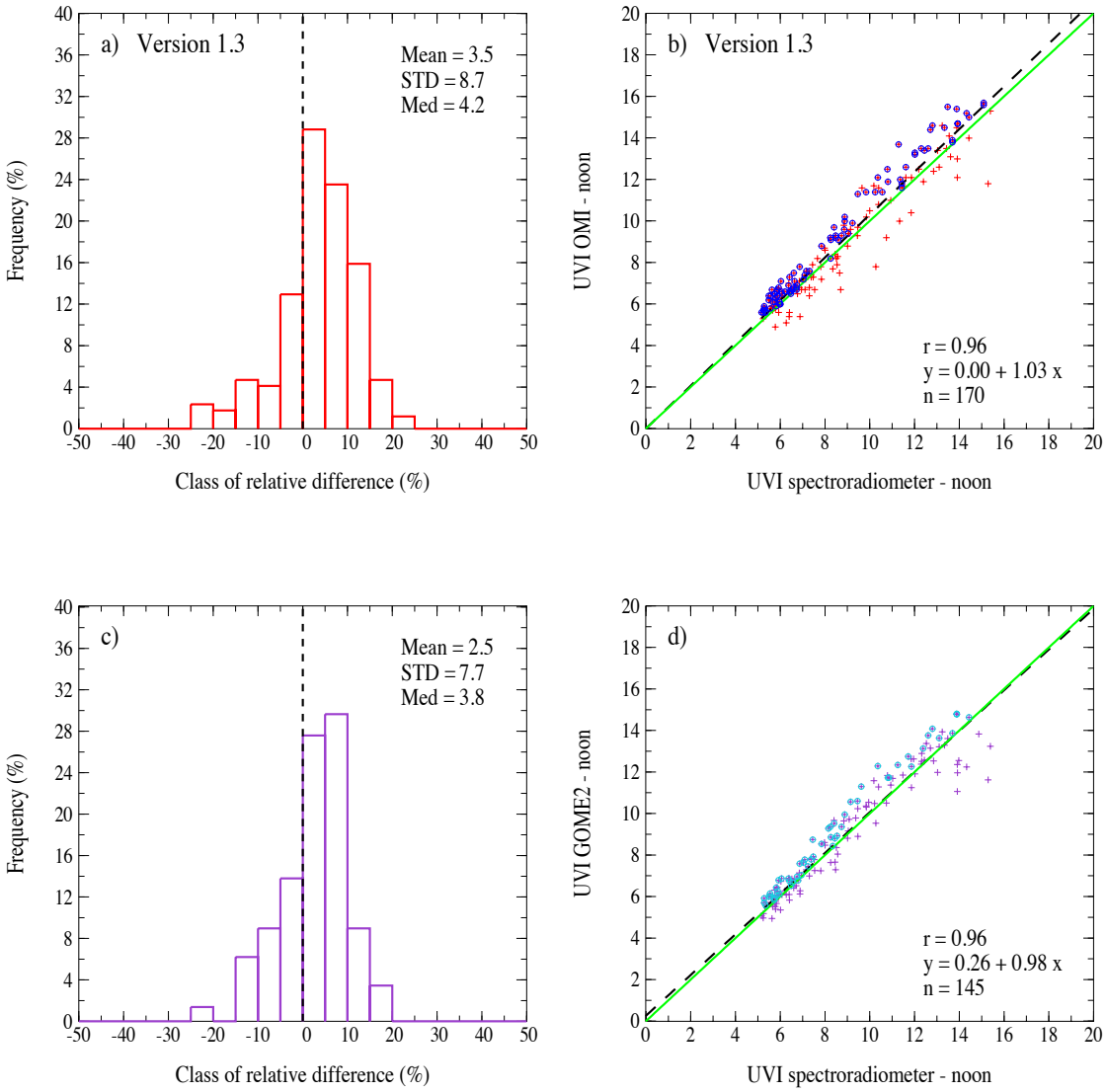

Figure 12. Same as Fig. 2 but for SDR. Percentiles for OMI: p_{10}=-7.9 %, p_{90}=13.7 %; for GOME-2: p_{10}=-8.1 %, p_{90}=10.6 %.

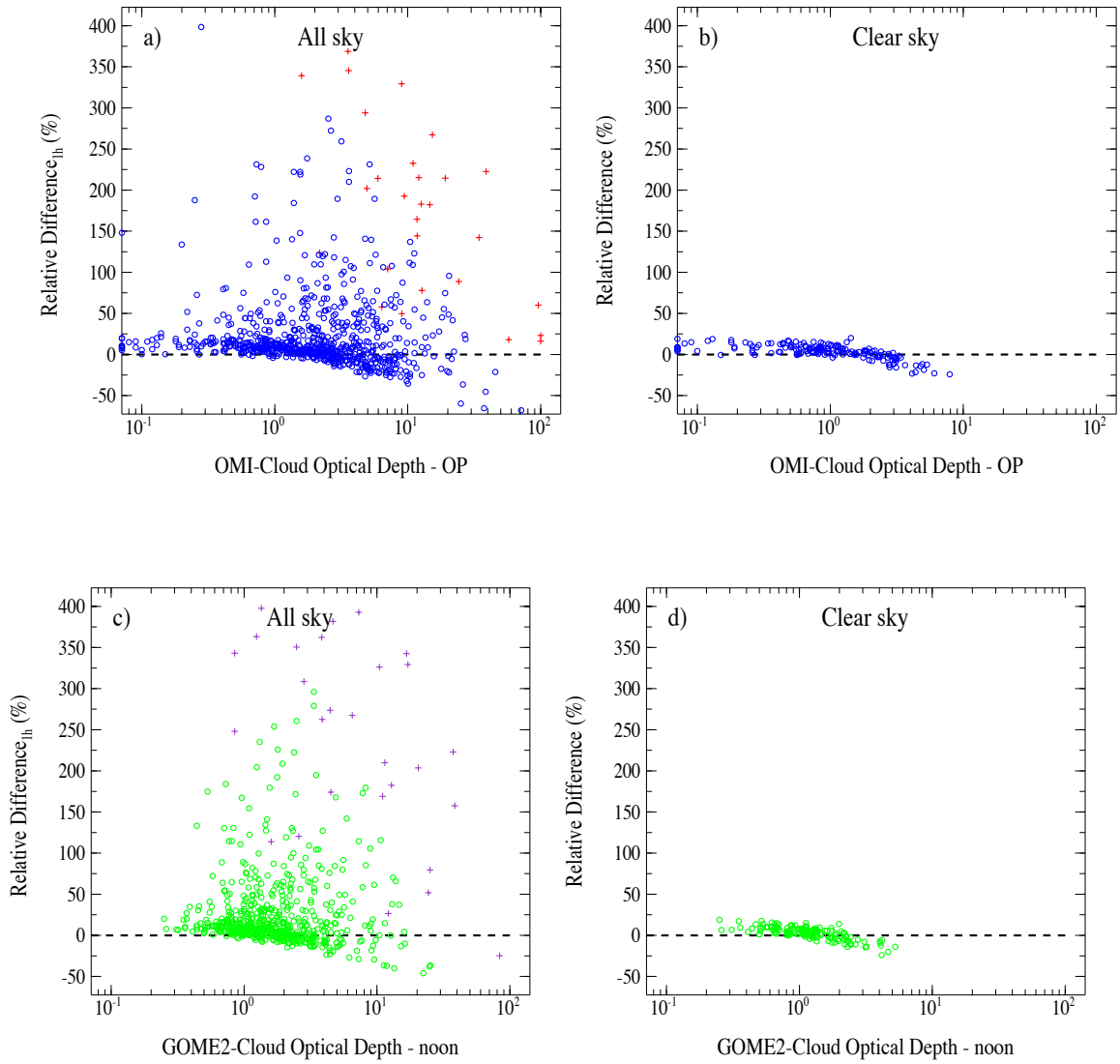

Figure 13. Same as Fig. 3 but for SDR.